Renewable and Sustainable Energy Reviews 24 (2013) 288–305

Contents lists available at SciVerse ScienceDirect

Renewable and Sustainable Energy Reviews

journal homepage: www.elsevier.com/locate/rser

Nanoengineering thermoelectrics for 21st century: Energy harvesting and other trends in the field

Marisol Martín-González*, O. Caballero-Calero, P. Díaz-Chao

Instituto de Microelectrónica de Madrid (IMM-CNM-CSIC), c/Isaac newton 8, PTM 28760 Tres Cantos (Madrid), Spain

ARTICLE INFO

Article history:
Received 14 September 2012
Received in revised form
28 February 2013
Accepted 4 March 2013
Available online 16 April 2013

Keywords:
Thermoelectricity
Energy harvesting
Nano-structured materials

ABSTRACT

In the beginning of the 21st century, the world is facing the major challenge of finding energy sources to satisfy the ever-increasing energy consumption while preserving the environment. In the race to search alternative energy sources, thermoelectric generators are called to play their role in the improvement of the efficiency of the actual energy system by harvesting nowadays wasted heat. This review deals with the novel aspects of nano-structuring of thermoelectric materials, from the so called 3D nanobulk materials down to the incorporation of 0D quantum dots in thermoelectric structures. The improvement in the efficiency of nanoengineering thermoelectrics benefits mainly from the reduction in the thermal conductivity. Other promising trends in thermoelectricity are also reviewed, such as, novel nano-structures, trending materials (polymers, thermionic materials or Zintl phases), spin caloritronics, thermoelectricity in atomic and molecular junctions, or recent developments in theoretical calculations. Finally the review ends with a brief review on recent thermoelectric devices.

Contents

1. Introduction

The ever-increasing amounts of electricity needed in everyday life and the well-known scarcity of fossil–fuel reserves, power the search for alternative energy sources as one of the major challenges of the 21st century. Much effort is being invested in this

* Corresponding author. Tel.: +34 918060700; fax: +34 918060701.
E-mail addresses: marisol@imm.cnm.csic.es (M. Martín-González), olga.caballero@imm.cnm.csic.es (O. Caballero-Calero).

1364-0321/$ - see front matter
http://dx.doi.org/10.1016/j.rser.2013.03.008

direction, intensified by the impact that the carbon-based combustion is causing in the environment. However, considering the enormity of the problem every effort is welcome, so that not only research on potential resources to substitute fossil fuels (such as photovoltaics, wind power technology or hydrogen-based technologies) must be encouraged, but also research lines devoted to improve the current fuel efficiencies must be followed. Nowadays, most of the energy produced in our society is lost in terms of heat, mainly in electrical power generation and transport. For instance, from the electrical energy for consumption in our houses, around 60% of the energy extracted from power plants is lost as waste heat during its generation [1], and between 8% and 15% is lost as heat in the electrical lines for its transport and transformation [2]. Therefore, only ~35% of the energy produced in a power plant reaches our houses. Another example is the efficiency that is obtained in transportation, where 40% of the energy produced in a car is wasted as heat and another 30% of the total is used for cooling the engine, making a total of 70% of wasted energy, and this without taking into account the CO_2 emissions to the atmosphere produced by this extra 70% of petrol that has to be used. It is in this scenario where thermoelectric materials can contribute to be part of the solution to have a more sustainable world, taking advantage of their ability to convert temperature differences into electrical power, that is, obtaining power from wasted heat.

Thermoelectric devices also present the advantage of not having moving parts, which makes them more silent and easier to maintain over time if compared with other energy sources. A clear example of their durability without maintenance can be found in the thermoelectric devices that the NASA's spacecrafts Voyager 1 and 2 use as main resource of their electrical power since 1977, when they were launched, and which continue working and sending data to earth 35 years later. Another advantage is their easy miniaturization, which makes them suitable for their integration in small devices, such as watches, transmitters, etc. Also, these devices can be used for cooling and heating applications, since by passing an electrical current through the devices they generate a difference in temperature. Uses range from simple food, wine cabinets or beverage coolers for a picnic to extremely sophisticated temperature control systems in space vehicles, infrared detectors, or missiles.

The goodness of a material in terms of thermoelectricity is given by the Figure of Merit proposed by Altenkirch in 1909, $ZT=(S^2\cdot\sigma/\ \kappa)\cdot T$, where S is the Seebeck coefficient (the potential generated per degree of applied temperature difference), σ the electrical conductivity (the ability to conduct electricity), $\kappa=\kappa_e+\kappa_L$ the thermal conductivity (the ability to conduct heat energy by both the electrons, κ_e, and the lattice, κ_L, sometimes referred to as the phonon conductivity), and T the absolute temperature. Sometimes, in absence of thermal conductivity data, the $Power\ Factor=S^2\cdot\sigma$ can be used to give an idea of the goodness of a thermoelectric material. The Figure of Merit is directly related to the efficiency of the material as energy converter, being the main subject of research the improvement of the Figure of Merit of the currently available materials in order to make them competitive in the market. The relation between the Figure of Merit and the efficiency of a thermoelectric device is given by the following formula:

$$\eta(\%)=100\cdot\left(\frac{T_H-T_C}{T_H}\right)\cdot\frac{\sqrt{1+Z\overline{T}}-1}{\sqrt{1+Z\overline{T}}+(T_H/T_C)}$$

where η is the efficiency in %, T_H and T_C are the hot and cold temperature sides, respectively, and $Z\overline{T}$ is the Figure of Merit at the mean temperature. The variation of the efficiency as a function of the hot temperature can be found in Fig. 1 for several values of ZT. It must be noted that the Seebeck coefficient, electrical conductivity and thermal conductivity in this formula are supposed to be constant in the whole temperature range. Fig. 1a shows the efficiency of a device which works with the cold side at a constant temperature of 0 °C. This situation, however, is rather unlikely since, in practice, it is very difficult to maintain the cold side fixed at 0 °C or even at (27 °C), being more common to have the cold side at a temperature higher than room temperature (RT, usually taken as 27 °C). It is worth mentioning that this is not usually taken into account, and that is what present Fig. 1b and c, where the impact on

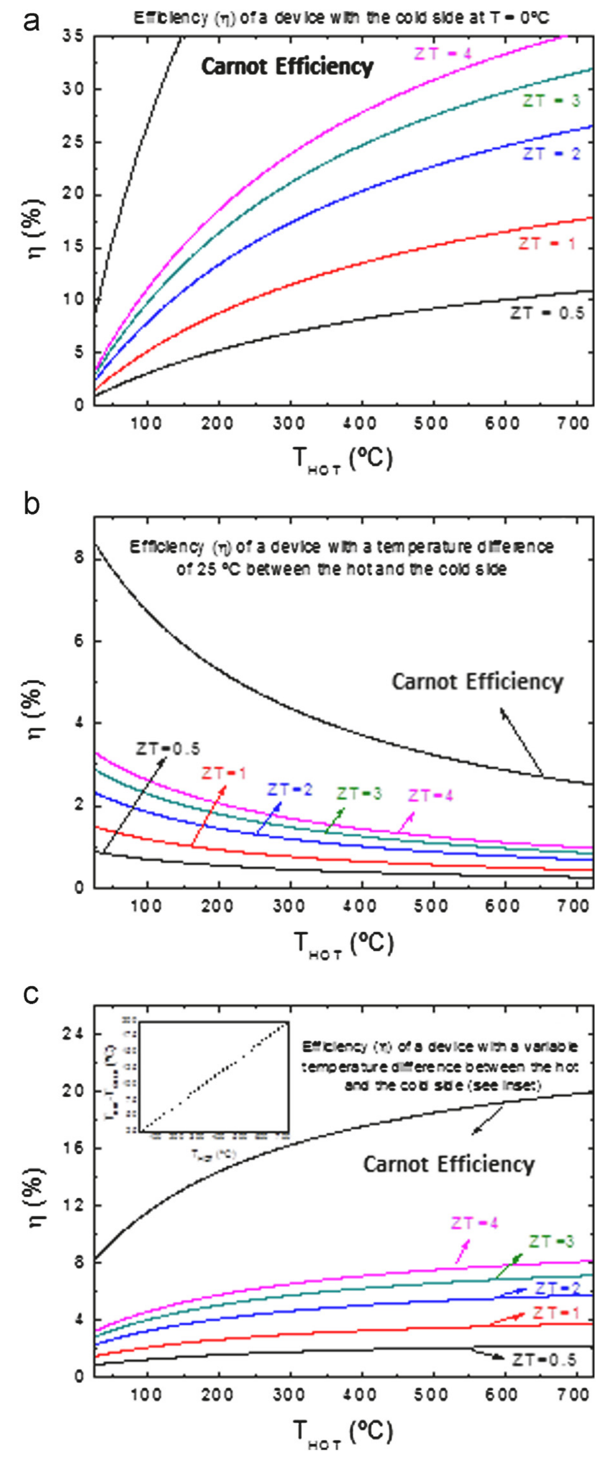


Fig. 1. Efficiency of a thermoelectric device as a function of the hot temperature for various values of the ZT is shown. The cold side is assumed to be at (a) a fixed temperature $T=0$ °C, (b) a variable temperature (see ΔT in the inset), and (c) 25 °C below the temperature of the hot side (TH).

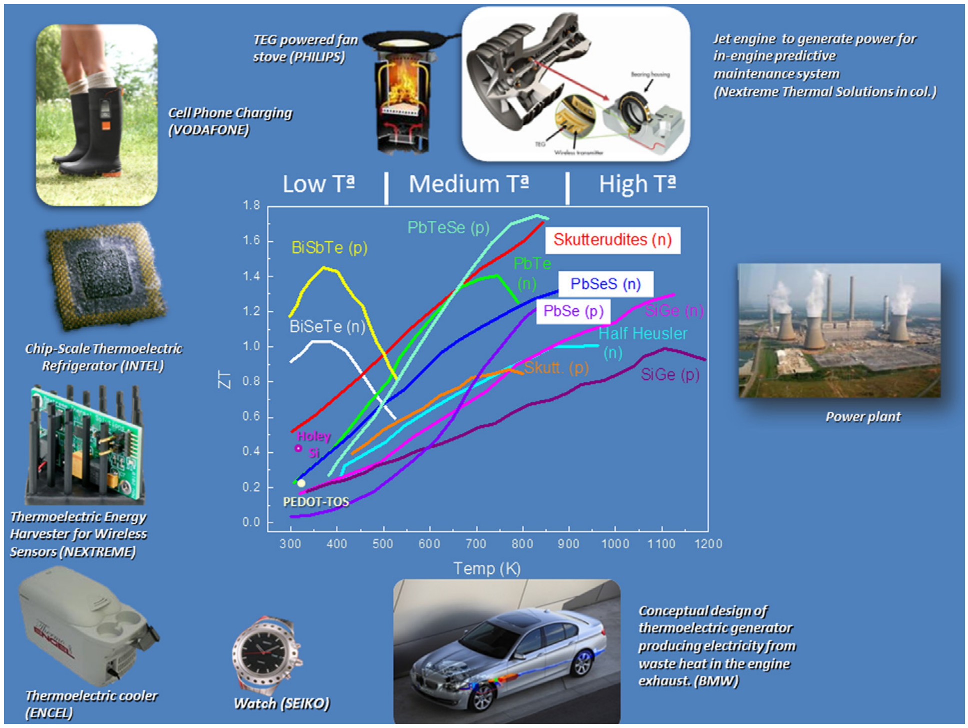


Fig. 2. Summary of the main applications of thermoelectric devices depending on their working temperature range. Also the best materials for each range to date are displayed. The white bars mark the limits for each temperature range.

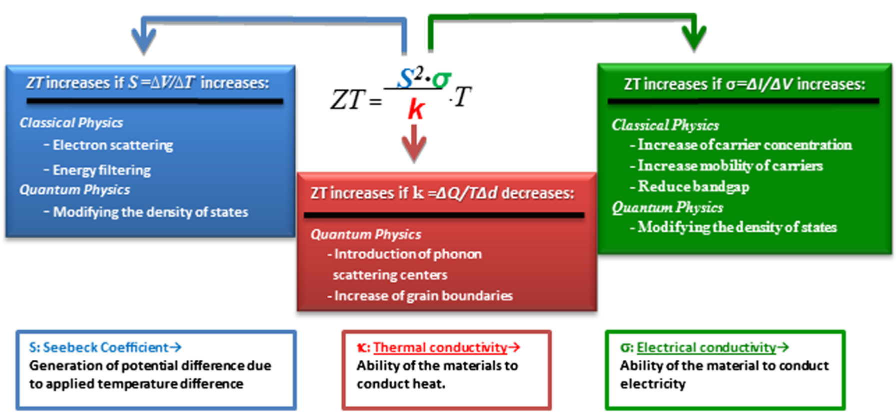


Fig. 3. Different approaches to increase the Figure of Merit *ZT* of thermoelectric materials taking into account classical physics or quantum physics.

the efficiency of a device when the temperature of the cold side increases from RT is shown. This gives a more realistic view of what could be achievable by a TE device. In the case of Fig. 1b, a constant difference of temperature of 25 °C has been assumed between the hot and the cold side. In Fig. 1c, a variable temperature difference is considered (shown in the inset of Fig. 1c).

Nowadays, the highest *ZT* values obtained are starting to get higher than 1. The target *ZT* that would make these devices interesting for more than only niche applications is a *ZT* of 2 or higher. Furthermore, as it is shown in Fig. 1a–c, keeping the cold side as low as possible is also of great importance to allow a high performance of the thermoelectric devices.

Nowadays, examples of applications for these materials are scarce, but some examples of power generating devices based on thermoelectric materials which are now on the market are summarized in Fig. 2. For example, some low temperature devices are consumer lighting/power, industrial sensors and building automation. In this temperature range, the most commonly used materials are Bi_2Te_3 based alloys. Nevertheless, new materials are under study such as polymers [3] or silicon with nanosize pores [4], which *ZT* values are starting to be very interesting for future applications. In the medium to high temperature range devices for cook stoves, turbine sensor power, jet engine bearing sensors or vehicle exhaust gas heat recovery power systems among others, are commercialized or in demonstration stages. For this temperature range the best materials right now are PbTe based alloys, which contain lead (the lead content is why the PbTe is of low interest for applications within Europe due to the RoHS directive, which includes lead on the list of Hazardous Chemicals). For high temperature applications Skutterudites, SiGe alloys and Half-Heusler compounds are the best choices at this moment. The applications within this temperature range are found mainly in recovering industrial wasted heat. All these informations are summarized in Fig. 2.

Therefore, in order to improve the material's thermoelectric performance, the *ZT* must be increased [5] (see Fig. 3) enlarging the electrical conductivity (improving the conduction of electric

current in the material, increasing the mobility of electrons and reducing its bandgap, for example), lowering the thermal conductivity (usually its lattice contribution κ_L is more easily tuned by the introduction of interfaces), or increasing the Seebeck coefficient, for instance by electron scattering or energy filtering.

Historically, the first materials studied in the frame of thermoelectricity were metals, when the Seebeck effect and the Peltier effect were discovered in the 19th century [6]. Soon, it was shown that the efficiency of metals was quite low compared to that of semiconductors, especially those with low bandgap which present higher Seebeck coefficient. Nevertheless, there is a main drawback to improve the Figure of Merit, which is that the coefficients S, κ_e and σ in classical physics are interrelated, in such a way that it is not possible to increase one without affecting the others. Therefore, a compromise has to be reached to find the maximum ZT value. In this sense three different strategies have appeared in order to improve the ZT: (a) looking for new materials with complex band structures, like heavy fermion compounds (this approach increases (↑)S while keeping the values of σ and κ_e); (b) controlling the disorder in materials that can be considered electron crystals and phonon glasses, like Skutterudites or Clathrates. These materials present a rattling effect which causes, ↑σ and decreases (↓)κ_l see for instance ref. [7]; and (c) nano-structuring , that could lead to ↑S due to quantum confinement effects, while ↓κ_l due to the scattering of phonons at the interfaces. This last approximation constitutes the main subject for this review, because it is the main reason for the latest improvements in the Figure of Merit of different materials.

The appearance of new physical phenomena at low dimensions is now being under extensive study as a way to allow an independent control of both S and σ. In the first theoretical predictions, the main responsible of this tunability was the change that the density of electronic states presents when quantum confinement takes place [8]. In addition to this theoretical enhancement of the power factor, the reduction of dimensionality plays a role on decreasing the thermal conductivity due to the increasing phonon scattering in the greater number of interfaces that low dimensional materials present when compared with normal bulk configuration (see Fig. 3).

There already are some interesting reviews on thermoelectricity [9–15] that focus on a particular group of materials. There are also other works that covered the state-of-the-art in this area when they were published [16]. However, the ever-increasing literature on thermoelectricity makes it difficult to remain updated, and that is why we present this new work. In this review, we will try to summarize and update some of the main strategies that are being followed nowadays to produce efficient thermoelectric devices with higher performance via nano-structuring in 3, 2, 1, and 0 dimensions. It should be highlighted that the main advances obtained so far have arisen from tailoring the lattice thermal conductivity, κ_L, which is independent of the other relevant parameters present in ZT [17]. For a more detailed explanation of the effect that nano-structuring has in the electronic band structure, density of states, barrier layers in superlattices see [9,18–20].

2. Nano-structuring of thermoelectrics

In a theoretical paper by Dresselhaus and Hicks [21], that appeared in 1993, it was suggested that miniaturization would affect the thermoelectric properties once the quantum regime is reached, producing an enhancement in the Figure of Merit ZT. In Fig. 4b, extracted from this paper, the calculated ZT is depicted for bismuth telluride, showing a dramatic increase when reducing the dimensionality from 3D (volume) to 2D (thin films or superlattices), and to 1D (nanowires) (see Fig. 4c). This initial work has powered the field over the last years. Many scientists have tried to look for the predicted enhancements and, as a result, exciting and innovative breakthroughs have appeared.

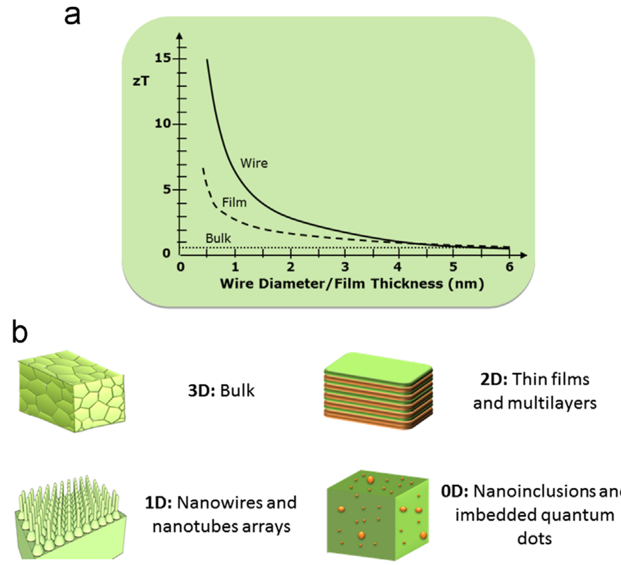


Fig. 4. (a) Simplified sketch of a thermoelectric device and (b) theoretical calculations of how the dimensionality and size of the structure affect the ZT value for bismuth telluride (extracted from Ref. [21]). (c) Examples of different nano-structuring with different dimensionalities.

The first studies carried out to confirm the effect of quantum confinement effects in the density of states were done in 2D superlattices, consisting on PbTe quantum wells of less than 4 nm width and $Pb_{1-x}Eu_xTe$ barriers [22]. The good agreement with the calculations produced a great interest in novel ways of designing and growing superlattices to improve the Figure of Merit adjustment of bulk thermoelectric materials (see Section 2.2).

As a natural way of lowering the dimensionality, studies on 1D quantum wires (Section 2.3) and 0D quantum dots imbedded in certain matrices or nanoinclusions (Section 2.4) were performed. However, the original theory does not strictly apply to the 0D case, since the calculated enhancement in the power factor for quantum-confined 1D and 2D structures occurs in the perpendicular direction to the confinement, and this direction has no sense for 0D structures.

To date, an increase in ZT has been found in some cases in which nano-structuring has been performed. It seems to be generally accepted that these increases are more related, so far, to a reduction of the thermal conductivity (because of the phonon scattering at the nano-structure interfaces), than to an increase of the Seebeck coefficient. Some groups are working nowadays in underlying the physics at the nanoscale for this type of materials, and these new efforts are summarized in the theoretical predictions of Section 3 at the end of this review.

Based on this decrease of κ_L due to phonon scattering, there has been a whole new branch of research devoted to 3D nanoengineered bulk materials. Those are materials that present nanoscale features (nanograins, for instance, which increase the number of interfaces), which give them a lower thermal conductivity than the normal bulk material. Although these are the most recently investigated materials from a historical point of view, this paper will start with them, under the title of 3D nano-structured materials. Then we will refer to lower dimension structured materials (2D, 1D and 0D) and we will review the more recent achievements in each of these structures. Finally, we will make a

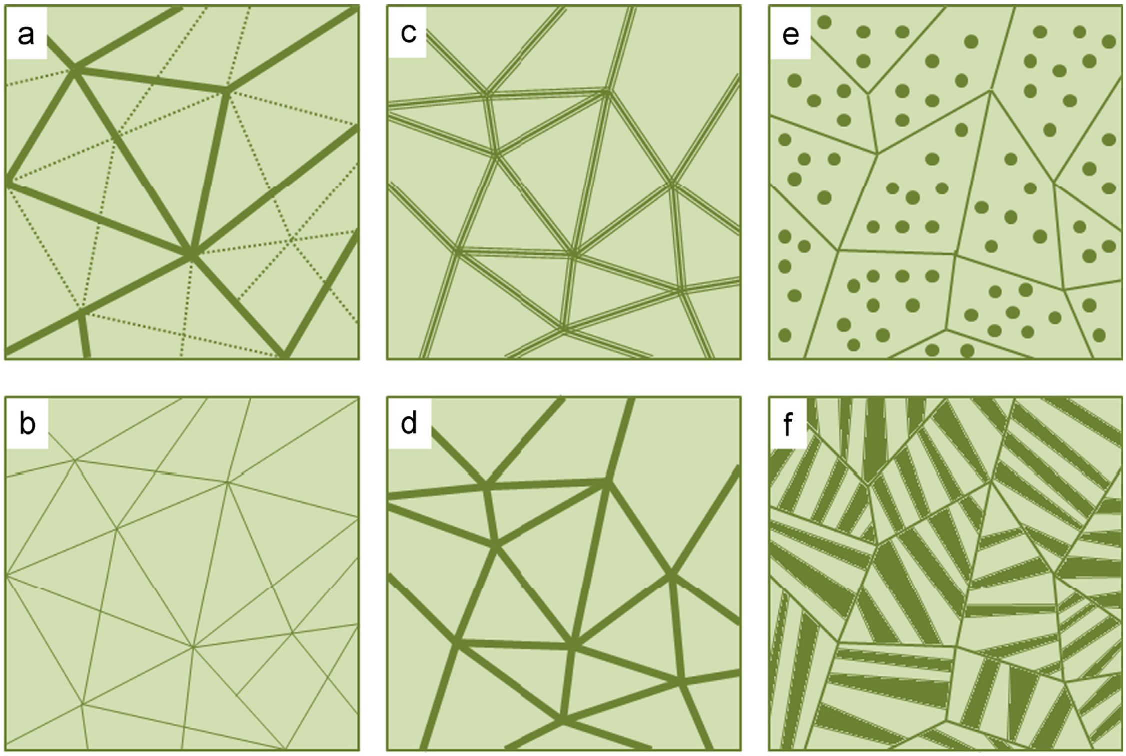


Fig. 5. Different nano-structured bulk materials: (a) and (b) refer to structures consisting on one material but (a) with a polycrystalline nano-structure and (b) compacted nanograins. (c), (d), (e) and (f) refer to structures formed by two or more materials, being (c) grains coated with another material, (d) bulk material with nanoinclusions in the grain boundaries, (e) grains with nanometric inclusions, and (f) multi-layered grains. Adapted from Ref. [23].

brief outlook on other interesting trends that have been arousing in the field of thermoelectricity in the last years.

2.1. Nano-structured bulk thermoelectrics

Nano-structured bulk materials (NBM) have been developed quite recently. They are able to combine low dimensional characteristics along with the production of bulk samples, which makes them easier to handle and shape. This is a great advantage, since most of the standard measurement techniques have been developed for bulk samples. Moreover, all the industry fabricating thermoelectric devices is based on bulk samples. So, if a NBM appeared with really high *ZT* it would, in principle, be easier and faster to be introduced in the market than other low dimensional structures.

Those NBM can refer to different structures. On the one hand, bulk samples that contain nanometric inclusions and, on the other hand, materials that present a heterostructure in the form of nanoparticles of the same compound (such as polycrystalline nano-structures or compacted nanograins) or different compounds (such as grains coated with another material, bulk material with nanoinclusions, grains with nanometer inclusions, or multi-layered structures). In principle, in all these cases, the number of interfaces is greatly increased compared to the normal bulk material (see Fig. 5). In addition, it has been experimentally shown [8] that the performance of heterogeneous nanoparticle compounds or compounds with nanoparticle inclusions are higher than the performance of an alloy of two constituents. In this way, the importance to preserve the nanostructures during the processing is obvious, not only to maintain the number of boundaries, but also to conserve the stoichiometry of the nanoparticles.

NBM provide a way to increase the scattering of phonons without affecting strongly the electrical charge transport. This effect produces a lowering of the thermal conductivity of the lattice, κ_L, over a wide temperature range, without interfering too much with the value of the electrical conductivity [8,23]. This end, which may not be intuitive, has been demonstrated from a theoretical point of view [24]. A simplistic way of understanding it is to imagine a nano-structured medium in which the electrical carriers can find a path of lower resistivity and make their way along the bulk (through percolation effect). In the case of phonons, they do not have such an option, because they find obstacles in each boundary which scatter them and, thus, reduce the thermal conductivity.

However, there is not yet a complete understanding of the reason why the thermoelectric capabilities are increased in some nanocomposite materials while in others it is not. There has been a big advance in understanding the phonon transport, but the carrier transport behavior is still not well understood, in particular in those cases with many interfaces or complex nano-structures with several scattering mechanisms [19,20].

Although the theory behind their thermoelectric performance is still to be improved, there has been a lot of experimental research on NBM. To fabricate them, nanometric precursors plus reactive SPS can be used or nanoparticles of the desired thermoelectric materials must be produced. The nanoparticles are usually made via wet chemical methods that can be used for the production of different nanostructures of thermoelectric materials [25], hydrothermal methods, inert-gas condensation methods or ball-milling [8]. Once the nanoparticles are obtained, they can be compiled into a solid by different techniques, such as sintering, spark-plasma sintering (SPS), hot pressing (HP) cold pressing, plasma pressure compaction (P^2C), extrusion, etc. A review of how these techniques are applied to thermoelectric materials can be found in Ref. [26].

As a first example of dense and strong bulk nanocomposites that arise from pressed nanoparticles of a single material, one can take Si based alloys (Si_xGe_{1-x}), which have been used as bulk thermoelectric materials in the past for the space aircraft missions, providing a *ZT* around 0.5 for p-type and nearly 1 for n-type at 900 °C. The measurement of the Figure of Merit after

compacting nanograins of p-type $Si_{80}Ge_{20}$ obtained through ball-milling and compressed into a solid by hot pressing has given values of $ZT=0.95$ at around 900 °C [27]. In the case of n-type $Si_{80}Ge_{20}P_2$ nano-structured bulk, a ZT value of 1.3 at 900 °C has been achieved following the same preparation method [28]. The explanation of these improvements is mainly due to the different mean free paths that electrons and phonons present in this material [28].

One of the traditional and most studied thermoelectric materials for room temperature applications is Bi_2Te_3, which, consequently, has been one of the first to be transformed into bulk nano-structures to improve its ZT [26]. In 2008, disk shaped samples were obtained from high purity powders of Bi and Te, milled in a 2:3 rate and then compressed via spark-plasma sintering. In those samples, a ZT of 1.2 at 150 °C was obtained [29]. In the search to improve these nanocomposites by tailoring the size of the nanoparticles, a two-step synthesis process has been developed, which is able to prepare nanoparticles of Bi_2Te_3 under 10 nm radius [30], obtaining a reduction of the thermal conductivity by a factor of ~2 at −73 °C, increasing up to an order of magnitude at low temperatures (~ −250 °C). Further improvements have been made with Bi_2Te_3-based compounds, for example $Bi_xSb_{2-x}Te_3$, for which nanometer-size powder was prepared by hot pressing, with a reported ZT of 1.4 at 100 °C [31]. This value was increased, afterwards to a ZT of 1.56 at 30 °C with a method of melting, quenching, annealing and spark-plasma sintering from a bulk nano-structured $Bi_{0.52}Sb_{1.48}Te_3$ [32]. Moreover, there are studies that show, from a theoretical point of view, that a change in the concentration of the different elements can lead to an optimal compound such as $(Sb_{0.75}Bi_{0.25})_2Te_3$, which could reach a ZT value as high as 1.8 at 27 °C [33].

Another material which has been considered for nano-structuring is PbTe, which exhibits a ZT of 0.7 at around 400 °C. In Ref [34] is observed an increase of S in nano-structured PbTe with inclusions of EuTe prepared by conventional metallurgical treatments, such as ball milling, and then pressed and sintered. The authors study the dependence of the Seebeck coefficient in terms of a *scattering parameter* (λ), that depends on the scattering mechanism of the carriers (interaction with phonons, impurities, etc.) and that controls the energy dispersion relation. Further studies show that PbTe can be modified including an excess of lead as nanometre size metallic nanoparticles (~30 nm) [35]. This lead precipitates, producing an enhancement of the Seebeck coefficient when compared to bulk PbTe [36]. In another different approach the synthesis of 100–150 nm spherical PbTe nanocrystals is presented via solution-phase and then spark-plasma sintering [37] obtaining an enhancement of S, but with an overall ZT of 0.1 at RT, very similar to the value of bulk samples. The given explanation for this effect is that the sintering methods on PbTe nanopowder produce an increase on the size of the nanograins, giving rise to grains not smaller than 1 μm in the final composite, leading to the same properties of the bulk compound [26]. Among the efforts to maintain the size of the grains after the sintering, one of the approaches is the use of thallium to dope the PbTe and introduce impurity levels that allow a ZT value of 1.5 at 500 °C for bulk nano-structured $Tl_{0.02}Pb_{0.98}Te$ [38]. Very recently, several works have reported improved values of the ZT up to 1.8 at 525 °C and 575 °C in PbTe–PbS [39] and PbTe–PbSe [40] alloys, respectively, that are able to successfully combine the distortion of the density of states through the doping with Na and the reduction of the thermal conductivity with the aid of nano-structuring. Detailed transmission electron microscope studies on the PbTe–PbS 12% samples revealed precipitates of 1–10 nm and 100 nm size of the PbS phase, in which the Na presence plays an important role being the responsible of the phonon scattering.

$AgSbTe_2$ is a compound that is more likely to be found mixed with other phases, such as SiGe (named TAGS, with a ZT of 1.2 at 150 °C) than by itself, due to the apparition of segregated phases with little loss of its stoichiometry. It has an extremely low thermal conductivity (0.63 W/m K at RT), which makes it a very interesting material for thermoelectric applications. In 2008, H. Wang et al. [41] prepared this compound by mechanical alloying and spark-plasma sintering obtaining a ZT value of 1.59 at 300 °C, and a reduced thermal conductivity of 0.3 W/m · K at room temperature. In 2010, Xu et al. explored a new synthesis route involving sonochemistry and SPS, obtaining similar results to the previously reported by Wang (ZT of 1.55 at 260 °C [42]). Very recently, another work reported slightly enhanced values of the ZT up to 1.65 at 300 °C introducing nanopores of 5–10 nm in the bulk prepared by melt spinning and SPS [43].

As mentioned above, the $AgSbTe_2$ is usually found as a constituent of other phases. In particular the mixing of the $AgSbTe_2$ with the cubic PbTe has given rise to a new material, known as LAST (Lead, Antimony, Silver and Tellurium, $AgPb_mSb_nTe_{2+m}$), which reaches a bulk ZT value around 1. This compound presents nanoinclusions that act in a similar way to the quantum dots in the case of superlattices of $PbSe_{0.98}Te_{0.02}$/PbTe (see Section 2.2). They have a complex crystalline structure, based on the NaCl lattice (Na is substituted by Ag, Pb and Sb; and Cl substituted by Te) with electronic and structural distortions, which lead to a reduction of κ_L. Moreover, through a change of their composition (varying m and n) both the carrier concentration and the electrical conductivity can be tailored obtaining n-type and p-type materials. The nano-structuration of this material was introduced by Kanatzdis in the year 2004, where the fabrication method was a melting followed by a really slow cooling, in order to obtain the nanocomposite material with a lot of nanoscale inhomogeneities within the PbTe matrix. The reported Figure of Merit was $ZT=2.1$ at 530 °C [44], and even though later experiments obtained lower values, around 1.5 and 1.7, a lot of research is being devoted to these materials nowadays [45–47]. Preparation of LASTs via mechanical alloying and spark-plasma sintering has reverted in values of ZT of 1.37 at 400 °C [45] and newer research substituting silver with sodium [48] or potassium based LASTs [49] have shown values of 1.7 at 375 °C and 1.6 at 475 °C, respectively.

One more promising family of novel thermoelectric materials is Skutterudites, with a $CoAs_3$ type structure. In general, they are formed by a transition-metal such as cobalt, rhodium or iridium, along with a second element such as phosphorous, arsenic or antimony with the formula MX_3, being M the transition metal and X the other element. The high Seebeck coefficient and electrical conductivity that exhibit the Skutterudites make them quite attractive for thermoelectric applications. Another advantage that they present is their reduced production cost, due to the elements that constitute these materials, compared to other classical thermoelectric compounds [50]. Although, they have a rather high thermal conductivity, this has been successfully overcome by filling the voids of the centre of their unit cell with large-mass and small diameter interstitials (Ca, Sr, Ba, La, Nd, Cr, etc.) which produce a rattling effect, increasing the phonon scattering and thus reducing the thermal conductivity. Values of ZT as high as 1.1 at 480 °C with p-type $Ce_{0.28}Fe_{1.5}Co_{2.5}Sb_{12}$ and ZT 1.25 at 630 °C with n-type $Ba_{0.3}Ni_{0.05}Co_{3.95}Sb_{12}$ have been reported [51]. The best ZT value in this kind of material up to date is 1.7 at 577 °C, in the $Ba_uLa_vYb_wCo_4Sb_{12}$ multiple-filled Skutterudites [52]. The last improvements in these materials concern their fabrication, which has started to be made with a melt-quench method to fabricate $CoSb_3$ Skutterudites doped with both In and Ce, with reported ZT values of 1.43 at 530 °C [53].

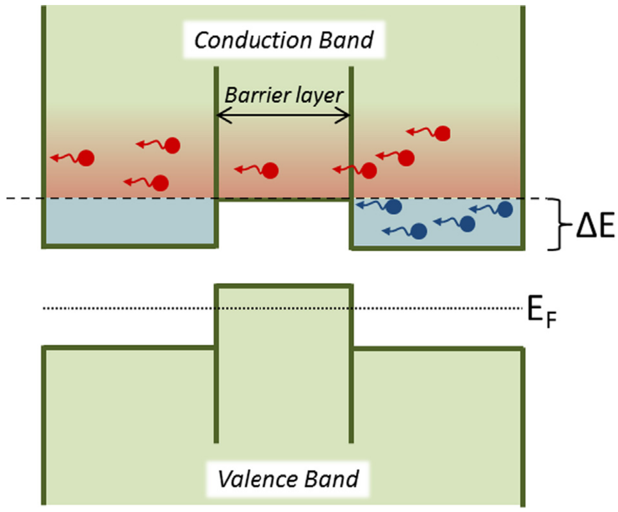


Fig. 6. Schematic representation of the energy filtering effect. This picture represents the particular case of the half-Heusler (HH) alloys with nanoinclusions of full-Heusler alloys (FH). Adapted from [60].

In the case of nano-structured Skutterudites, nanoparticles have been fabricated via hydrothermal synthesis and then bulk $CoSb_3$ has been prepared by spark-plasma sintering or hot pressing [54]. Moderate *ZT* values of 0.7 in n-type $Co_{0.8}Ni_{0.2}Sb_3$ at 500 °C nanocomposites have been already achieved [55]. There are also studies on $CoSb_3$ modified with fullerene additions which are synthesized by SPS [56], creating new grain barriers due to the presence of C_{60} that affect the carrier scattering and produce an increase of the *ZT* value of bare Skutterudites. Also nanosize oxides have been introduced in the bulk matrix of $CoSb_3$ such as Yb_2O_3 nanoprecipitates, or CeO_2 nanoparticles, among other oxides [57].

Half-Heusler (HH) compounds are other low cost and thermoelectrically efficient materials. They crystallize in the MgAgAs structure and are more environmentally friendly than LAST or PbTe systems. They present a narrow bandgap along with a density of states with a sharp shape near the Fermi level. *ZT* values reported for these materials range from 0.8 at 530 °C for $Hf_{0.75}Zr_{0.25}Ni_{0.9}Pd_{0.1}Sn_{0.975}Sb_{0.0025}$ to 1.4 at 430 °C for $(Zr_{0.5}Hf_{0.5})_{0.5}Ti_{0.5}NiSn_{1-y}Sb_y$ [58]. In principle the obstacle for their use as efficient thermoelectric materials is their high thermal conductivity, what gives them much room for improvement with the aid of nano-structuring. For the moment, there has not been much increase in their Figure of Merit due to nano-structuring. Nevertheless, some improvements have been recently reported with an enhanced *ZT* of 1 at 600–700 °C. This has been achieved in nano-structured bulk samples prepared by hot pressing of nanopowders of $Hf_{0.75}Zr_{0.25}NiSn_{0.99}Sb_{0.01}$ [59]. Another approach that has been followed is the use of the "energy filtering" effect. The concept of energy filtering is based on the introduction of barriers of 1–10 times k_BT in the valence band for p-type materials or in the conduction band in the case of n-type materials. These barriers prevent the transmission of low energy carriers, which cannot surpass them, and that is why this effect is called "energy filtering", because it filters the carriers with lower energies (Fig. 6). Thus, the conduction is only due to the carriers with higher energy (also called ``hot`` carriers). This results into an increase of the Seebeck coefficient, due to the fact that its value is related to the thermal energy of the carriers. The total thermal energy becomes higher once the ``cold`` carriers have been removed and only the ``hot`` ones are left. In the case of the Half-Heusler (HH) nano-structured compounds, these are prepared with nanoinclusions of Full-Heusler alloys (FH) that act as an energy filter for the low energy electrons, remaining the high energy electrons almost unaffected. With this method, the HH alloy ($Zr_{0.25}Hf_{0.75}NiSn$) has been prepared with sub-10 nm scale nanoinclusions of the FH alloy ($Zr_{0.25}Hf_0.75Ni_2Sn$), obtaining an enhancement of a 100% in the power factor (~3.5×10^{-3} W/m K^2) [60].

2.2. 2D: thin films and superlattices

In order to have access to any possible quantum effects, the dimensionality has to be reduced in films (Fig. 4b) so that thicknesses of the films are in the order of tens of nanometres, depending on the material.

The nano-structures in which it has been most extensivey studied the effect of quantum confinement in 2D are the superlattices. They consist in alternating layers of different components with thicknesses in the nanometre scale. These structures were firstly introduced by Esaki and Tsu in 1970 [61] who studied them as ultra-high-frequency oscillators. They were proposed for thermoelectric purposes in 1998 [62], based on the principle of *carrier pocket engineering*. In a general way, the purpose of the layers is to block the phonons of the lattice, thus reducing the heat flow, without stopping the flow of electrons. It is possible to further reduce the thermal conductivity in phonon scattering centres added to the structure, for instance, at the interfaces. But this is just the classical way of increasing the *ZT* by decreasing the thermal conductivity. In order to take advantage of quantum effects in these structures, the layer thicknesses should be reduced to a point where the electronic band structure is affected by the size of the films, and quantum wells are formed.

One of the most well-known results in these structures is the one reported in 1997 by Venkatasubramanian et al. [63]. They fabricated via metalorganic chemical vapor deposition (MOCVD) alternating layers of Bi_2Te_3 and Sb_2Te_3 with periods from 1 to 8 nm. All those films were *c*-oriented and were bonded to each other by van der Waals forces, which prevented bismuth or antimony to diffuse to the different layers because of the low bonding force. The reported *ZT* was an impressive 2.0 at 27 °C, that was some years later enhanced up to *ZT*=2.4–27 °C (300 K), which is the maximum *ZT* obtained so far in this system [64]. The measurements, however, were performed using the Harman method, what implies that they have been done in the out-of-plane direction, and since the quantum effects in Dresselhaus' model are expected in the direction perpendicular to the confined dimension, this high *ZT* value cannot be understood within such model. Nowadays, some of these interesting results are being tried to be reproduced worldwide without much success so far, which may be an indicator of the difficulty to stabilize these complicated structures. Other groups, which have studied also the cross-plane transport in Bi_2Te_3/Sb_2Te_3 superlattices, have also demonstrated that the reduction of the thermal conductivity due to the phonon scattering at the interfaces is the main cause of improvement in the Figure of Merit of those systems [37,38]. The greater effect of the reduction of the thermal conductivity in the Figure of Merit than that of the power factor was also concluded in the investigation carried out in $Bi_2Te_3/Bi_2(Se_xTe_{1-x})_3$ superlattices [65].

Other extensively studied superlattices are those made of lead salt films. In all those cases, the enhancement of the Figure of Merit is due to a reduction of the thermal conductivity. Some of these superlattice structures fabricated by MBE are PbTe/$PbSe_{0.2}Te_{0.8}$ (with a maximum *ZT* of 1.2 at 230 °C) [65], and PbTe/$Pb_{0.93}Eu_{0.07}Te$ quantum-well structures [22]. In the case of PbTe/PbSe heterostructures, the main experimental problem was the lattice mismatch between both layers, which resulted in PbSe quantum-dot structures between the PbTe layers instead of thin layers of PbSe. Some of these structures are $PbSe_{0.98}Te_{0.02}$/PbTe showing *ZT* values of 0.9 at 27 °C [66], and PbSeTe/PbTe quantum-

dot superlattices, all fabricated by MBE means [67,68], where values of *ZT* as high as 1.6 and ~3.0 at 27 °C and 300 °C, respectively, were obtained when Bi was used as n-type dopant.

Other interesting superlattices are those based on silicon, mainly because they can be envisioned as more easily integrated in chips, due to the development of silicon-based industry. In the Si/SiGe system, the enhancement of the Figure of Merit was demonstrated due to the quantum wells that Si forms [17]. In this case, there was a good agreement between experiment and theory, supporting the idea that quantum confinement effects in 2D is achievable in these systems. Moreover, Si/SiGe superlattices show higher power factors than SiGe alloys alone. However, when Si/SiGe superlattices and SiGe alloys are compared in the frame of an actual microrefrigerator device, both of them show the same cooling power [69]. This could be due to a higher thermal conductivity in the superlattice than in the bulk SiGe, making the superlattice structure comparable to the bulk in terms of thermoelectric efficiency, although this would go against the general believe that the introduction of interfaces does reduce the thermal conductivity.

In conclusion, in the 2D systems two ideas can be highlighted: firstly, there is a lack of metrology related with the measurement of the Figure of Merit in the out-of-plane configuration. The difficulties arising in these measurements come not only from the performance of good electrical contacts, but also from the establishment of a thermal gradient through a nanometric length and its accurate measurement. Secondly, the quantum confinement is still to be demonstrated, although there are certain results that show good agreement with the theoretical predicted values. Those conclusions, however, should be considered carefully since the Seebeck coefficient and electrical conductivity are measured in the film plane, but thermal conductivity is measured out of plane. In most cases, the effect of phonon scattering seems to play a more important role in the increase of the Figure of Merit than the possible quantum effect on the density of states.

2.3. 1D nanowires and nanotubes

According to the theoretical predictions shown in Fig. 4, the greatest quantum effect on the thermoelectric Figure of Merit would be found in the lowest dimension present in the graph, this is, 1D. Therefore, quantum wires of thermoelectric materials have been developed. The advantage of these structures is that when the diameter of the nanowires or nanotubes is decreased, the electronic density of states presents singularities which increase largely the density of states at certain energies (van Hove singularities). The aim, therefore, is to reduce the sizes of the nanowires enough to house just a few quantum states, causing a split in the energy bands that gives rise to discrete sub-bands. In that way, the semiconductor can become a semimetal in practice. Some of the most studied materials in the form of 1D structures have been Bi and Bi-based compounds. Actually, the first experimental observations of quantum confinement effects were performed in Bi nanowires. In 1998, Heremans et al. suggested the observance of quantum confinement effects in the magnetoresistance of Bi nanowires of 200 nm in anodic alumina templates prepared by a vacuum evaporation technique [70]. Moreover, the same year, Dresselhaus et al. prepared Bi nanowires employing vacuum melting bismuth on top of commercial porous alumina of several diameter pores followed by a pressure injection process [71]. In this work they reported a semimetal to semiconductor transition when reducing the diameter of the wires that was consistent with the theoretical predictions of a transition driven by quantum confinement effects. The reason why bismuth was chosen is that, due to its semi-metallic nature, the size-quantization effects affect both the conduction and valence band and, therefore, decreasing the diameter of the nanowires below 50 nm (which is achievable using alumina templates) a gap appears between both bands. This produces a transition to semiconductor-like behavior, which is more easily observable than such effects in other properties and therefore the quantum confinement can be easily recognized. In the case of nanowires of Bi_2Te_3, for example, it is predicted that for diameters smaller than 30 nm one should start to see an increase in *S* due to quantum confinement [72], along with a reduction in the thermal conductivity because of phonon scattering in the surface of the nanowires. Conceptually, the template-assisted nanowires growth is simple and intuitive. Also, in order to have a final device, the nanowires should be inside a matrix so they have mechanical stability and a high density of them. In the case of alumina $> 10^{10}$ nanowires/cm^2 can be obtained. Also it is important the tunability of the diameter of the template. In porous alumina different sizes from 400 nm to 15 nm can be achieved as reported in literature [73,74]. Some examples of anodized alumina templates normally fabricated in our laboratory are shown on Fig. 7.

Several thermoelectric materials have been prepared inside alumina templates [75] and also inside polycarbonate membranes (another interesting template for nanowires) [76] by different methods. Among them, we will start with electrochemical deposition [77]. The advantages of this technique are, for instance, the high deposition rates achievable at cost-efficiency (without vacuum systems or expensive facilities), the easy scalability for industrial applications, and also that the process is usually carried out at room temperature, which produces a reduction of the thermal stress in the samples. All these characteristics are crucial for their future commercialization.

In order to fabricate nanowire structures via electrochemical deposition, it is mandatory to study firstly the fabrication of films with this technique, allowing a way to find the optimal parameters to obtain the deposited material with the desired composition, homogeneity and quality. A good review on the status of the thermoelectric films grown by electrodeposition can be found on reference [77]. Once the films have been optimized and the proper growth parameters are known, these conditions can be applied to the growth of nanowires [78]. Several materials have been successfully electrodeposited in films, such as Bi [79], $Bi_{1-x}Sb_x$ [80], Bi_2Te_3 [81,82], PbTe [83], Bi_2Se_3 [84], $Bi_{1-x}Sb_x$ [85], and $CoSb_3$ [86], among others. A summary on the preparation of nanowires arrays by electrodeposition is shown in Table 1.

As shown in Table 1, the most thoroughly studied material in the case of 1D nano-structures obtained by electrodeposition is bismuth telluride. In this case, diameters down to 25 nm in porous alumina matrices and lengths of around 60 μm [87] have been reached.

In the case of one-dimensional thermoelectric materials, one can note that there is not much data about the Figure of Merit of the different structures. It is worth to mention here the difficulty involved in the measurement of the thermoelectric properties in the case of nanowires.

Measurements of the performance of isolated Bi_2Te_3 nanowires have been performed with suspended micro-chips [88], or with the Harman method in 200 nm wires, giving values of *ZT* of 0.82 [89]. In that work it has been observed that the Figure of Merit decreases with time due to an oxidation layer that forms in the surface of the wire. This decay, along with the fact that out of 40 nanowires measured only three presented measurable *ZT*, points out one of the main difficulties measuring single nanowires, that is, the oxide formation on its surface [89]. To prevent this oxidation of the nanowires, the thermoelectric properties should be measured without taking them out of the alumina matrix, as it has been made with the thermal diffusivity of 40 nm diameter Bi_2Te_3 nanowires embedded in amorphous alumina in Ref. [90], where a photo-thermal technique was used showing a reduction

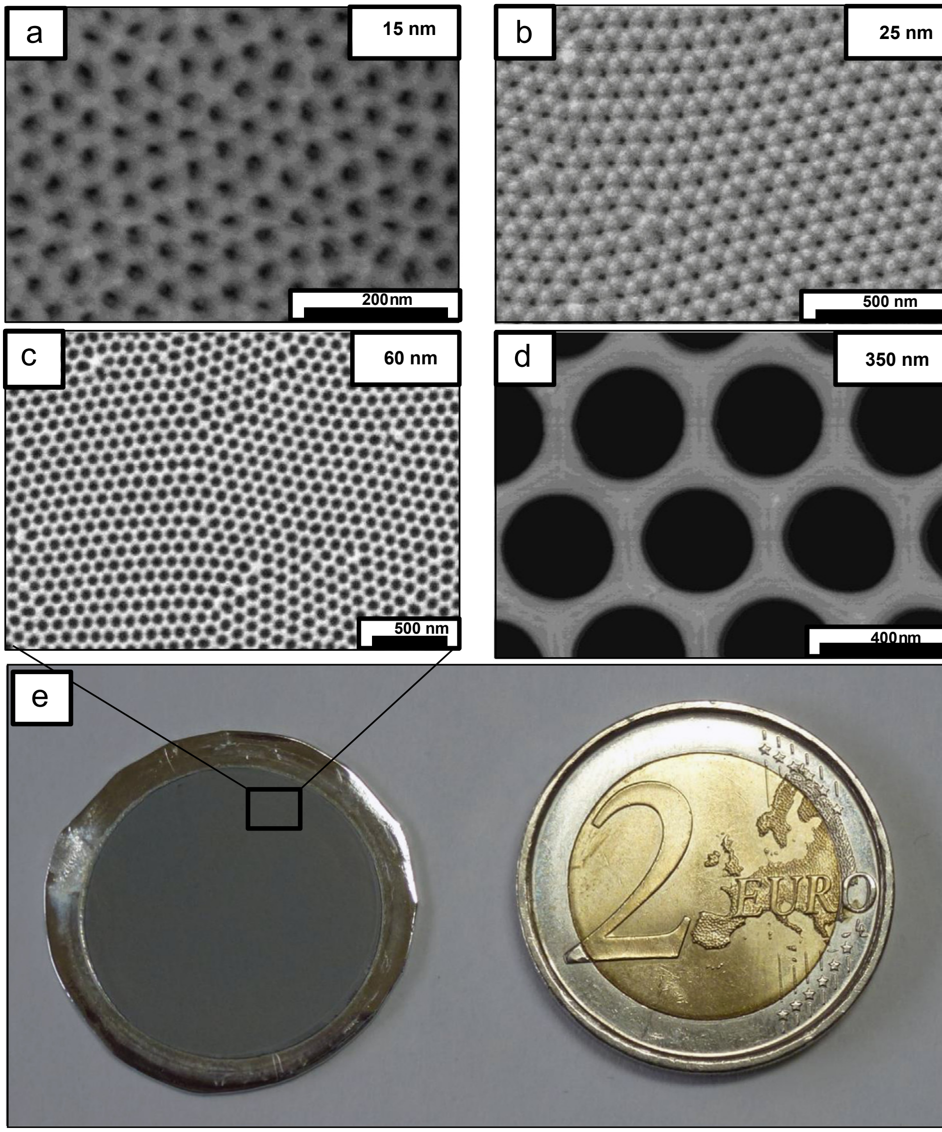


Fig. 7. Different porous alumina templates synthesized by anodization in our laboratory [73,74] with porous diameters of (a) 15 nm, (b) 25 nm, (c) 60 nm, and (d) 350 nm. In (e) the comparison between a whole porous alumina template and a two euro coin can be seen.

of the thermal conductivity of one order of magnitude compared with bulk Bi_2Te_3. In a more recent work, a gold layer was electrochemically deposited on the end of the wires to prevent further oxidation, and the measurements were made the aid of an atomic force microscope (AFM). The value of the Seebeck coefficient along with the electrical conductivity was obtained [91], but an accurate measurement of the thermal conductivity is yet to be implemented. Other reports on electrodeposited p-type bismuth telluride nanowire arrays (diameters of 120 nm) include measurements of the thermal conductivity, and give a value of *ZT* of 0.9 at 80 °C [92]. It is important to note that the diameters of these wires are not small enough to reach the quantum confinement effect, so any expected improvement of the Figure of Merit should come from the reduction of the thermal conductivity. However, as it occurs in the case of Bi_2Te_3 electrodeposited films, the Seebeck coefficient and the electrical conductivity of Bi_2Te_3 electrodeposited nanowires are lower than those exhibited the bulk or by other high vacuum techniques. This is probably due to the fact that the perfect optimization of the materials has not yet been achieved by this method. More work should be done in this direction.

Given the interest that attracts the bismuth telluride and its alloys from a thermoelectric point of view, other type of 1D nanostructure has been prepared. In particular, in 2005, it was shown that this material can be obtained in the form of nanotubes [93]. With this structure, it presents the advantages of the low-dimensionality of the walls along with the hollow structure of the tube, which should lead to an increase in the scattering of phonons in the tubes without affecting much the electrical conductivity, given that electrical current can be transported along the walls. These Bi_2Te_3 nanotubes were prepared by hydrothermal synthesis, obtaining tubes with a few microns length and 30–100 nm in diameter with spiral tube-walls. Then, to make practical devices, this nano-structured powder was mixed with n-type Bi_2Te_3 at a ratio 15:85, and then hot pressed at 350 °C for 30 min in vacuum at 50 MPa of pressure. The calculated *ZT* for this structure improved slightly the value found for bulk Bi_2Te_3 up to ~1 at 450 K for the state-of-the-art at the moment.

Nanowires have also been made of other materials such as silicon, showing that although bulk Si is a poor thermoelectric material (*ZT* around 0.01 at room temperature), nano-structuring can lead to an increase in the phonon scattering and thus, reduce the thermal conductivity and increase the thermoelectric Figure of Merit up to values of ~1.0 at −75 °C for nanowires with 20 nm in diameter and ~0.3 at RT for nanowires 10 nm wide [94]. In this

Table 1
Summary of some of the most important works on electrodeposited thermoelectric nanowires arrays.

TE material	Theoretical prediction	Template	Experimental observations
Bi	Semimetal-to-semiconductor transition at $\phi\sim50$ nm depending on the crystal orientation [166–168]	Polycarbonate	Among the first to synthesize and electrically characterize electrodeposited Bi nanowires [76,169,170]
	For 5 nm Bi nanowires oriented along the trigonal axis at 77 K, a maximum ZT of 6 with an optimized carrier concentration 10^{18} cm was predicted [167]	Alumina	Single crystal [171–174]
$Bi_{1-x}Sb_x$	ZT of 1.25–1.5 for 35–45 nm diameter nanowires of 10–15 at % Sb [175]	Alumina	$\phi\sim200$ nm, DMSO is used as a solvent for the first time [80]
		Alumina	$\phi\sim40$ nm [176]
		Alumina	Bi/Sb superlattice [177]
		Polycarbonate	$\phi\sim20$–100 nm [178]
Bi_2Te_3	ZT enhancement for nanowires of less than 10 nm through enhanced charge carrier mobility by quantum confinement effects [21]	Alumina	$\phi\sim200$ nm [179]
		Alumina	$\phi\sim40$ nm, first work on lab-made alumina templates [180]
		Alumina	$\phi\sim25$ nm [87,181]
		Alumina	$\phi\sim15$ nm [182]
		Alumina	$\phi\sim15$ nm [183]
		Alumina	pulse electrodeposition [184]
		Alumina	core/shell polyaniline/Bi_2Te_3 nanowires [172]
		Highly oriented pyrolytic graphite (HOPG)	step edge decoration [89]
$(Bi_{1-x}Sb_x)_2Te_3$		Alumina	First time it was obtained. $\phi\sim40$ nm. In this work also films are grown and the electrochemical reaction mechanism is presented [78]
		Alumina	$Bi_2Te_3/(Bi_{0.3}Sb_{0.7})_2Te_3$ superlattices [185]
Sb_2Te_3		Alumina	$\phi\sim50$ nm [174]
$Bi_2Te_{3-y}Se_y$		Alumina	First time it was obtained. $\phi\sim40$ nm. In this work also films are grown and the electrochemical reaction mechanism is presented [186]
$CoSb_3$		Alumina	$\phi\sim200$ nm nanowires [187]
		Alumina	$\phi\sim60$ nm nanowires [188]
PbTe		Alumina	High-filling rate and in large area are dense and continuous [83]
		Photoresist	$\phi\sim20$–100 nm [189]
$PbSe_{1-x}Te_x$		Alumina	$\phi\sim100$ nm nanorods [190]
InSb	Values of ZT higher than 1 for InSb nanowires with $\phi\sim10$ nm, and ZT up to 3 for $\phi\sim5$ nm [191]	Alumina	$\phi\sim50$ nm nanowires [192]

case, nanowire fabrication was carried out with the superlattice nanowire pattern transfer (SNAP) method, where the achieved enhancement of the *ZT* value was explained through the phonon drag effect (the phonon drag is a contribution to the Seebeck effect that is due to the phonon flow from the hot to the cold side of the samples that "push" the charge carriers, as its name suggests, to the colder side of the sample through the phonon–electron (phonon–hole) interaction). The explanation involves the increased roughness of the nanowires, which scatter mostly the phonon modes that mostly affect the thermal conductivity. The effect of roughness has been observed also in Silicon rough nanowires prepared via electroless etching in an aqueous solution of $AgNO_3$ and HF from a Si wafer, with diameters varying from 20 to 300 nm [95].

A different approach to the tailoring of the thermoelectric efficiency on nanowires is the fabrication of segmented nanowires, as shown in [96]. Here, GaAs/GaP nanowire superlattices were grown via laser- assisted catalytic growth of solid targets, and the diameter of the nanowire was controlled by metal-catalysed synthesis of vapor–liquid–solid (VLS) process. In theory, those nanowires should present high electrical conductivity along the length of the nanowires while blocking to a great extent the phonon transport by phonon scattering at the interfaces of the different layers. This phenomenon can be achieved due to the difference of the atomic masses of the constituents of each segment, as it is shown, for instance, in the phonon conductivity theory developed for Si/Ge superlattices nanowires in Ref. [97].

Also, in 2005 Qiu et al. [98] presented a novel method of growing nanorods of PbTe by sonoelectrochemistry. With this technique they show monodispersed PbTe nanorods with well controlled morphology, crystallinity and composition of the nanorods grown, obtaining diameters down to 10 nm and lengths of 100 nm without any template.

As an example of a possible way of implementation of the thermoelectric nanowires into practical devices, Lim et al. [99] have reported a procedure to obtain a nanodevice comprised of electrodeposited Bi_2Te_3 nanowires as n-type material and BiSbTe nanowires as p-type material, using two alumina templates with different diameter pore sizes: a commercial one with 200 nm and a home-made alumina template with 43 nm, see Fig. 8. The power factors of the corresponding thin films of these compounds obtained with the same preparation conditions were of $8.22\cdot10^{-4}$ W/m K^2 and $8.88\cdot10^{-4}$ W/m K^2, respectively, however, these properties were measured in the in plane direction, and since the nanowires are to be contacted from top to bottom and both compounds are anisotropic materials, the expected properties of the device should differ from this values. Unfortunately, neither characterization of the nanowire arrays nor the efficiency of the nanodevice was shown.

The latest piece of work that we would like to highlight in this section is the measurement of the electrical conductivity of $Bi_{0.3}Sb_{0.7}$ nanowires arrays prepared by electrodeposition into porous anodic alumina made by the Stacy group together with Marlow industries [100]. In this work, the nanowire/alumina composite was assembled into a hybrid nanowire-bulk thermoelectric device, and electrical measurements were used to calculate the *ZT* of the device. To assure good electrical contacts to all the nanowires, Ni was electrodeposited on top of them. The

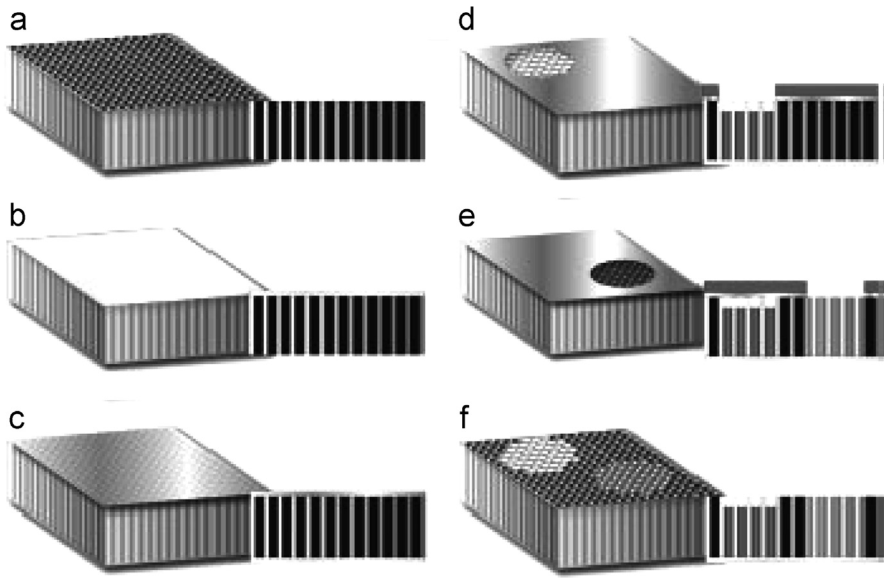


Fig. 8. Thermoelectric nanowire-based device fabrication process (main images: nanotemplate cut-out, insets: corresponding cross-sections). (a) Alumina nanotemplate; (b) nanotemplate sputtered with thin layer of gold as conduction and contact layer; (c) nanotemplate flipped over and mounted onto an Au/Ti substrate with silver paste followed by blanket deposition of parylene C; (d) first hole patterned in the sacrificial photoresist; the nanotemplate is exposed by oxygen reactive-ion etching and gold capped Bi_2Te_3 nanowires are electrochemically deposited; (e) after the planarization, processing steps are repeated to create the second hole opening, followed by $Bi_{2-x}Sb_xTe_3$ electrochemical deposition; (f) finished gold capped Bi_2Te_3 and $Bi_{2-x}Sb_xTe_3$ nanobundled elements ready for top and bottom interconnects (figure and footnote taken from Ref. [99]).

nanowire array produced a temperature difference of 7 °C and the hybrid couple had a *ZT* of 0.12, which is on par with an equivalent bulk couple. In this sense, more efforts should be made in optimizing the $Bi_{1-x}Sb_x$ nanowire arrays and also in achieving good thermal and electrical contacts.

It is remarkable that quantum confinement effects in electron magnetotransport and semimetal–semiconductor transition in Bi nanowires have been successfully observed. However, experimental results fail to indicate any significant enhancement on the *ZT* so far due to quantum confinement. These results can be explained taking into account the complexity in performing this type of measurements and the fact that much work should be put into optimizing the nanowire arrays and in their metrology. Furthermore, it should be noted that the reported values of the thermal conductivity of nanowires prepared with different diameters do not give coherent results, which vary from one order of magnitude [90] to only 20% lower than the bulk value [101]. Moreover, there is an important common conclusion in the works dealing with nanowires of reduced sizes, which is that the enhanced *ZT* values are achieved only due to the reduction of the thermal conductivity, being the theoretically predicted enhancement of the Seebeck coefficient and the electrical conductivity still to be observed. To achieve this enhancement it is mandatory to optimize the electrodeposition process and to go to smaller diameter sizes.

2.4. 0D quantum dots

Following the theoretical idea that by lowering the dimensionality higher thermoelectric performance can be achieved through the increase in the Seebeck coefficients (due to quantum confinement) and the reduction of thermal conductivity (due to the increase of the phonon scattering), there is also a trend to go down to 0 dimensions. From an experimental point of view, that means growing quantum dots of thermoelectric materials. It is obvious that the improvement of the thermoelectric effect must involve not only an increase in the Seebeck coefficient, but also a high electrical conductivity throughout the material. Therefore, the quantum dots cannot be electrically isolated, but embedded in conductive matrices. The common approach to introducing 0D in a thermoelectric system is to place quantum dots inside a bulk material, superlattices, or even nanowires.

In the case of superlattices, an example of structures with embedded quantum dots was already mentioned, when PbTe/PbSe heterostructures were described. There are many other cases where quantum dots have been incorporated to superlattices [67,68], and they are usually referred to as quantum-dot superlattices. The usual means of fabrication of these structures is MBE growth.

Another example of reduced dimensionality can be found in multi-layered nanowires. Some of these structures were fabricated via electrochemical deposition to study giant magnetoresistance [98], but the principle is the same for the fabrication of thermoelectric structures. In the case of the ref. [102], Si/SiGe nanowires were fabricated by a combination of chemical vapor deposition (CVD) and pulsed laser ablation, giving rise to ordered nanostructures along the nanowires. These structures were presented as promising from a thermoelectrical point of view, due to possible quantum effects. Nevertheless, the measurement of their thermal conductivity presents a similar dependence with temperature than in the case of Si/SiGe superlattices, which suggests that the main process involved in the increase of their efficiency is the scattering of phonons in the SiGe layers, along with scattering in the boundaries [103].

The general result of introducing quantum dots or 0D structures inside other thermoelectric structures or materials is an increase in the total Figure of Merit. However, this enhancement has not yet been proved to be a quantum effect, but a result of decreasing the thermal conductivity of the lattice by increasing the number of boundaries and defects in the material. In 2009, Kim et al. [104] studied the influence of the dimensionality on the performance of the thermoelectric devices. The main conclusion was that reducing dimensionality does not guarantee the enhancement of the efficiency; the important features are the shape and magnitude of the transmission channels, which depend also on the density of the nano-structures and their sizes. In this way, small quantum wells (0D) and wires (1D) are needed to

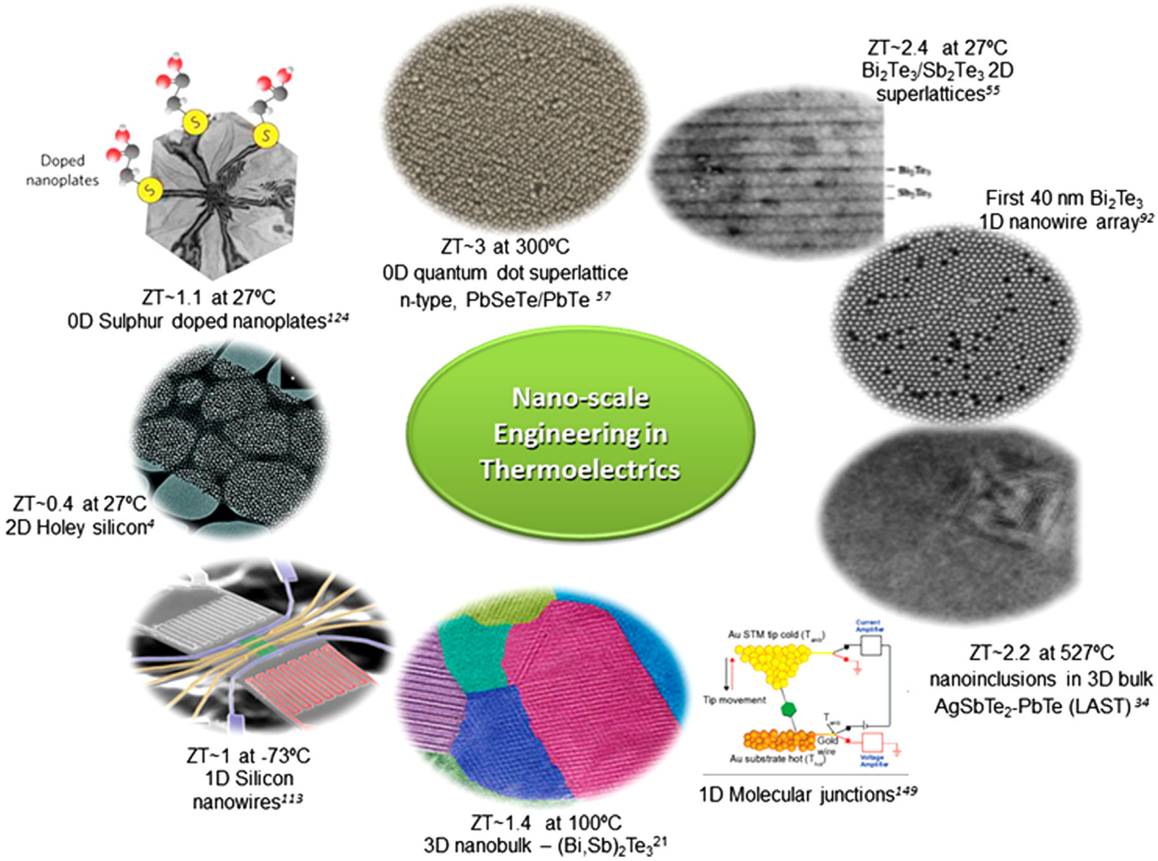


Fig. 9. Thermoelectricity in nano-scale materials: some of the main achievements.

increase the packing density and the proper thicknesses in the case of films (2D) have to be chosen to achieve any possible improvement of the 3D efficiency.

A summary of some of the best results so far in nano-structuring of thermoelectric materials is shown in Fig. 9.

3. Other trending topics in the field

So far, we have reviewed the most common materials where nano-structuring is being applied and higher *ZT* values are being achieved. There are other materials, however, where much effort is being invested and which are pushing hard to become trending topics in thermoelectricity. This is the case of novel nano-structures, such as polymeric materials, thermionic materials, spin-dependent Seebeck materials or Zintl phases.

3.1. Novel nano-structures

An interesting and quite recent development which is worth mentioning for its originality and properties is the novel concept of holey silicon. It was reported by Yu et al. [105] and Tang et al. [4] in 2010, and by Hopkins et al. [106] in 2011. This novel structure is the “negative” image of a nanowire array and it consists of a thin silicon membrane in which holes of a few nanometres (down to ~32–34 nm) in diameter have been made via lithography. These works show a highly reduced thermal conductivity, especially in the in-plane configuration (down to κ = 1.14 W/m K), without affecting much the electrical conductivity and the Seebeck coefficient. This reduced value of κ gives rise to a value of *ZT* = 0.4 at room temperature.

Very recently, Dechaumphai and Chen [107] published a theoretical work where they show that the classical incoherent phonon boundary scattering within the Boltzmann transport equation does not explain the obtained value of the in-plane thermal conductivity in holey silicon. Dechaumphai and Chen present a model that explains the experimental data, where the phonons with a mean free path lower than the distance between holes are treated like particles, while the phonons with a mean free path higher than this distance are interpreted as waves. An important conclusion of their work is that further reduction of the diameter of the holes and the distance between holes would yield a further reduced thermal conductivity.

Future research in this field aims to nanoparticle design. Novel chemical roots are being employed in obtaining new nanoparticles of thermoelectric materials. In this direction Mehta et al. [108] have demonstrated that p- and n-type bulk nanomaterials with an enhanced *ZT* of 1.1 at room temperature can be obtained using a bottom-up wet chemical synthesis followed by a sintering process by conventional methods. It is interesting that the reported improvement of the Figure of Merit is due not only to the usual reduction of the thermal conductivity because of the nano-structuring, but it is also due to an enhancement of the power factor produced by sulfur doping, which appears as a consequence of the preparation method. In these structures, the achieved *ZT* means an improvement of the 25% with respect to the corresponding bulk material.

3.2. Polymers

Organic polymeric materials constitute a recent growing topic in thermoelectricity thanks to their easier process of preparation when compared to that of inorganic materials, their cheap price in some cases, their high flexibilty, and the easyness to tune their properties with simple changes in their molecular structures.

Besides, they are considered environmentally friendly. The organic polymers, however, present an important drawback, which is their thermal instability at high temperatures, so they are limited to near-room-temperature applications. Among the immense number of organic polymers studied nowadays, the ones that present the most suitable properties for thermoelectrical applications are the conjugate polymers, such as polyacetylene [109], polyaniline (PANI) [110], polycarbazoles [111], or polythiophenes [3,111,112]. All these families of polymers have the common property of showing metal or semiconductor-like conduction with a very low thermal conductivity ($\kappa < 1$ W/m K), which makes them very interesting materials for thermoelectric applications.

The conducting polymers attracted great attention mainly since the development of the polyacetylene in 1977 [113], a discovery which earned Heeger, MacDiarmid and Shirakawa the Nobel Prize in the year 2000. They observed that when doping the polyacetylene with iodine atoms its conductivity increased 10 million times. Several years later, in 1991, Zuzok et al. [109] reported a slightly enhanced Seebeck of this material leading to a power factor of $\sim 10^{-3}$ W/m K, a value which is of the same order than that of the Bi_2Te_3. This polymer, however, is insoluble and unstable in air, which makes difficult to deal with it in practical applications.

The polyaniline (PANI) is another widely studied polymer since 1980 (see for example ref. [114]). It is a more stable polymer than the polyacetilene, but with a lower electrical conductivity ($\sigma \sim 600$ S cm^{-1}). It has been doped with many compounds, among which the one doped with hydrochloric acid presents the highest $ZT = 2.67 \times 10^{-4}$ at $T = 150$ °C in bulk samples [110]. Hostler et al. [128] reported an enhanced Figure of Merit of the PANI when doped with CSA (camphorsulphonic acid) reaching a $ZT \sim 10^{-3}$ at room temperature [115]. This value of ZT has been further increased in PANI films prepared by a stretching process, so that the alignment of the molecular chains produces an improvement of the carrier mobility, leading to a $ZT \sim 0.01$ at $T = 72$ °C [116].

The polycarbazoles are a family of polymers in which the carbazole unit may be linked to many positions in the main chain, what gives them a wide range of synthetic routes to easily modify their properties. They have been extensively studied for their promising properties in optoelectronics and light-emitting diodes, and recently their thermoelectric properties have been explored. Among the known polymers, the poly(2,7 carbazole)-based are the most promising ones for thermoelectric applications since they exhibit the largest power factor known in pristine polymers (~ 19 μW/m K) [111], with a Seebeck coefficient of ~ 34 μV/K and an electrical conductivity of ~ 160 S/cm, that gives a ZT on the order of 10^{-2} at room temperature. The fact of exhibiting this value of ZT without any doping or nano-structuring makes the future of poly-carbaloze based compounds very promising for thermoelectric applications.

Another highly stable polymer is the poly (3,4-ethylenedioxythiofene), known as PEDOT, which has also been widely investigated for a number of applications, such as photovoltaics [117], sensors [118], bioelectronics [119], electroluminescent devices [120] or thermoelectric [3]. When PEDOT is doped with poly (styrenesulfonate) (PSS), the electrical conductivity shows values as high as 600 S cm^{-1} and a very low thermal conductivity ($\kappa = 0.34$ W/m K) [121]. However, the low Seebeck coefficient ($S \sim 15$ μV/K) results in a poor power factor ($PF = 1.04 \times 10^{-5}$ W/m K^2) and a $ZT = 9.2 \times 10^{-3}$ at room temperature, which is two orders of magnitude lower than the reference inorganic materials. Nevertheless, a recent work by Bubnova et al. [3] shows that when the polyanion PSS is exchanged by small anions, such as tosylate (Tos), the resulting films of PEDOT:Tos exhibit an enhanced Seebeck coefficient ~ 210 μV/K and an electrical conductivity of ~ 70 S cm^{-1}, that combined with the low value of the thermal conductivity of 0.33 W/m K gives a value of the Figure of Merit of $ZT = 0.25$ at room temperature [3]. This result is very impressive for a polymeric material, and makes them a real alternative to the existing inorganic compounds at room temperatures.

The nano-structuration involving polymeric materials has been carried out through the fabrication of inorganic materials/polymeric materials composites. In 2002, the power factor of $Bi_{0.5}Sb_{1.5}Te_3$ nanoparticles/PANI composites was reported to decrease from ~ 400 to ~ 100 μW/m K^2 as the PANI content increased from 1 to 7 wt.% due to the reduction in the electrical conductivity [122]. Nevertheless, such reduction for the 3 wt% PANI, for example, was only a factor of 2, so that, a decrease of one half in the thermal conductivity of the composite would lead to an increase of the Figure of Merit. Some years later, the above mentioned work of Hostler et al. [115] studied the properties of PANI with a 1 wt.% of ~ 10 nm size Bi nanoparticles. The resulting composites showed a slight increase of the ZT of the PANI alone, from $ZT \sim 10^{-3}$ to $ZT \sim 1.4 \times 10^{-3}$ at room temperature. Other works reporting inorganic nanoparticles embedded in PANI matrices are, for example, PANI/graphite composites with a ZT of ~ 1.4 at 120 °C [123] or PbTe/PANI nanopowders [124]. It is worth mentioning that although both of them reported enhanced properties of the polymeric part, none achieved improvements with respect to the inorganic material. Other composites are PEDOT:PSS with Te core nanorods with a ZT of 0.1 at RT [125] or PEDOT:PSS with Bi_2Te_3 nanoparticles [126], where n-type and p-type conduction were reported with power factors of 80 μW/m K^2 and 131 μW/m K^2 and ZT of 0.04 and 0.08 at room temperature, respectively. Bi_2Te_3 nanoparticles with a 5 wt% content of polythophene content has been also reported [127] showing a ZT of 0.18 at 200 °C, which is much lower than the inorganic material without polymeric addition.

Another novel idea in the field of polymers is the use of carbon nanotubes (CNT) for thermoelectric applications. This is interesting because they present in 2D a linear relation between E and k at the Fermi level instead of the common parabolic one, so they can even be considered as a quasi 1D system [36]. The carbon nanotubes have been extensively studied as part of polymers/CNT composites. In this way, the 1D feature of the CNTs can be combined with the low thermal conductivity of the polymer materials. In 2008, Yu et al. [128], reported a ZT of 0.006 at room temperature for CNT/poly (vinyl acetate) (PVA) for a 20 wt% of CNTs. Some years later, the same group studied the CNTs embedded in a mixture of PVA and PEDOT:PSS prepared in films [129], which exhibited an enhanced Power Factor up to 160 μW/m K^2 in the in-plane direction. The thermal conductivity was measured in the out-of-plane direction, giving a value of 0.2–0.4 W/m K, and it was roughly estimated in the in-plane direction to be between 1 and 10 W/m K, what would mean a ZT between 0.02 and 0.4 at room temperature. Meng et al. [130] tested the CNTs with PANI, reporting a ZT of 10^{-3} at room temperature with a power factor of 5×10^{-6} W/m K^2 and a thermal conductivity of $\kappa \sim 0.5$ W/m K. The same composites of CNTs/PANI were prepared by Yao et al. [131], with an enhanced power factor ($PF \sim 5 \times 10^{-6}$ W/m K^2) but a higher thermal conductivity ($\kappa \sim 1.5$ W/m K), which resulted in a ZT of ~ 0.004 at RT. However, the highest ZT reported for CNT/polymer composites was obtained using PEDOT:PSS as a polymeric matrix. These structures showed a value of $ZT \sim 0.02$ at room temperature for a 35 wt% of CNTs with a $PF \sim 25 \times 10^{-6}$ W/m K^2 and a $\kappa \sim 0.4$ [132]. In this work, the CNTs were tested imbedded in PEDOT:PSS and also in Arabic gum, which is an insulator, to study the role of the polymer, and in the second case much worse results were obtained.

It is remarkable that the higher enhancements achieved in the thermoelectric properties of polymeric materials, including the inorganic material/polymer composites and polymer/CNTs composites do not involve the nano-structuring that so good results have produced in the inorganic materials. This can be easily understood, since the great achievement of the reduction of dimensionality in traditional materials has come through the reduction of the thermal conductivity rather than due to the enhancement of the power factor because of quantum

confinement effects. If we consider that one of the great advantages of the organic compounds is, indeed, their extremely low values of thermal conductivity, little benefit could be expected from this procedure. Nevertheless, the works dealing with polymeric nano-structures do report enhanced Seebeck coefficient and electrical conductivity, although these improvements, in the case of polymeric materials, arise from the realignment of the molecular chains as in the afore mentioned case of the stretched PANI films. In this sense, the improvements achieved with molecular chain ordering face the problem that, in general, the transport path of the charge carriers in polymeric materials involves in most of the cases more than one molecular chain, being the conduction controlled not so much by the properties within the molecular chain, but by the charge transfer between chains, being their percolation a very important factor to take into account [133]. Actually, to characterize accurately the thermoelectric parameters of some molecules and to avoid the percolation factor, Reddy et al. have trapped the organic molecules between two electrodes with a temperature difference across them [134]. Moreover, in a recent work it was predicted for different DNA-like chains [135,136] that, under certain conditions, the Seebeck coefficient and Figure of Merit of a lead-DNA-lead junction can be two orders of magnitude higher than that of other single-molecule junctions studied so far, which are on the order of few μV/K. These high thermo-power values seem to appear from transport resonance effects, which can be tuned rather easily in DNA.

3.3. Thermionic materials

Thermionic devices can be used as energy generators [137] or refrigerators [138], just the same as the thermoelectric devices. They were originally developed as two parallel metal plates separated by a small evacuated space. The working principle is based in Richanson's equation for the electron current emitted by a metal with a certain work-function (which is related as the energy needed to "evaporate" the electron from the metal) at a certain temperature [138]. In this way, a cathode is placed in contact with a heat source that provides enough energy to the electrons of the metal to overcome the potential barrier and get to the cold anode. The anode is connected to the cathode through a load resistance, allowing the electrons to return again to the cathode. As in the thermoelectric case, if instead of a temperature difference a voltage is applied between the metal plates, an electron flow appears from the metal with the higher Fermi energy to the metal with the lower Fermi energy, producing in the process a cooling of the cathode. The problem of these devices is that the work-function of the available metals limits their use to high temperature applications ($T > 500$ K). In 1997, solid state heterojunctions were proposed as energy barriers in thermionic devices so that they were available for lower temperature applications [139]. In the case of refrigeration devices, they are known as heterostructure integrated thermionic (HIT) coolers. In the HITs, the barrier can be formed by a single layer or by multiple layers, as it is the case of superlattices. In the latter, Vashaee and Shakouri [140] predicted values of $ZT > 5$. However, studies by Radtke et al. [141], Ulrich et al. [142] and others [139], showed that the use of thermionic/energy filtering processes is not advantageous, since the improvement of the ZT is due to the reduction of the thermal conductivity as a result of the structure used as barrier layer. Some of the materials used to have thermionic effect are, for example, $Hg_{0.8}Cd_{0.2}Te/Hg_{0.2}Cd_{0.8}Te$ superlattices [140], InGaAs/InGaAsP [142] or (Zr,W)N/ScN [143].

3.4. Zintl phases

The Zintl compounds have a nominal composition of AM_2X_2, where A is an alkaline-earth or a rare-earth element, M is a transition-metal or a main-group element, and X comes from the groups 15, 14, or more rarely 13. However, due to their content in alkali and alkaline-earth elements they are commonly air-sensitive. They favorably crystallize in $ThCr_2Si_2$-type structure, exhibiting large unit cells and a combination of covalent and ionic bonds, which make them electron–crystal and phonon–glass materials, meaning that they have high electrical conductivity along with low thermal conductivity. These characteristics make them quite suitable for thermoelectric applications [144]. Some examples of this category are $Ca_{11}GaSb_9$, $SrZnSb_2$, $Yb_{11}GaSb_9$, and $Yb_{14}MnSb_{11}$ [145,146]. Following the idea of introducing interstitials and lattice distortions, we find the β-Zn_4Sb_3 compound, which has a high ZT of 1.3 at 402 °C [147] but with some severe drawbacks: firstly, it is very brittle, making it a compound with poor manufacturability [148] and secondly, and more important, it presents low thermal stability, with thermal degradation caused by Zn evaporation after thermal annealing process in vacuum at $T > 377$ °C [148–150]. Nevertheless, nano-structured samples of Zn_4Sb_3 doped with Cd and prepared by melt spinning and SPS reported recently an improved thermal stability with similar ZT values [151]. In the Zn–Sb system, the phase ZnSb has been also studied as a thermoelectric material. This ZnSb phase was originally reported in 1961 to have a ZT of 0.6 at 187 °C [152]. Very recently, further investigations to improve its Figure of Merit obtained a value of 0.9 at 277 °C for Cu doped ZnSb samples with Zn_3P_2 nanoparticles.

Another similar compound of the type AZn2Sb2 (A = Sr, Ca, Yb, Eu) [152] was first reported by Gascoin et al. in 2005 [153], resulting in ZT values of 0.35 at 450 °C for the SrZn2Sb2 [154], of 0.92 at 330 °C for the EuZn2Sb2, or 1.2 at 430 °C for YbCd2-*x*Zn*x*Sb2 with $x = 0.4$ [155].

3.5. Spin-Seebeck effect or spin-caloritronics

Over the last years, after the works published by Gravier et al. [156] who reported on the spin-dependent Peltier effect in nanowires, and Usida, et al. [157], who observed the spin-Seebeck effect induced by a temperature difference along a ferromagnetic slab, there has been an increasing interest in this subject. This new emerging field is bridging the gaps between spintronics, magnetism and thermoelectricity and it is called "spin caloritronics", although "(mesoscopic) heattronics" or "caloric transport" have also been suggested.

The spin-Seebeck effect refers to the new physics related to spin, charge and entropy/energy transport in bulk materials, nano-scale structures, and devices. This phenomenon occurs in some materials due to the different scattering mechanisms involved in the conduction of spin-up and spin-down electrons. In this way, when a temperature difference is applied, the drift force suffered by the electrons is different for the spin-up than for the spin-down electrons, and therefore a "spin current" is obtained in the material. This spin-dependent effect has been observed in metals [157], semiconductors [158] and insulators [159]. Jaworski et al. [160] have recently shown that the phonon–electron interaction (phonon drag) has an important role in the spin distribution, suggesting that proper phonon engineering, combined with magnetic effects, could be applied to produce applications such as spin-cooling or magnetically sensitive thermoelectric materials.

3.6. Recent theoretical predictions

Since Hicks and Dresselhaus [21] predicted the enhancement of the Figure of Merit as a result of the reduction of dimensionalities in thermoelectric materials, much research has been done towards its experimental demonstration.

However, in the very last years some authors have revisited the theory of the enhancement of the thermoelectric performance due to

quantum effects, giving rise to the opinion that such enhancement is not straightforward. Actually, there are other important factors that were not taken into account in the original work. In 2011, Cornett et al. [161] deduced that the enhancement of the Figure of Merit does not monotonically increase with the reduction of the diameter of InSb nanowires. Instead, it presents a minimum at a certain size from which the *ZT* is finally increased. They also extended this study to any material with similar characteristics [162], concluding that the non-monotonically enhancement of the Figure of Merit is a general feature. Then, the enhancement predicted by Hicks and Dresselhaus would only occur in certain materials with particular characteristics. Moreover, Neophitous and Kosina have performed calculations using an atomistic model in silicon nanowires of several diameters [163–165] reaching similar conclusions than Cornett et al., but with a fundamental difference: although for reduced diameters there could be an enhancement due to quantum confinement, the surface roughness scattering (SRS) of the charge carriers would kill any enhancements provided by the quantum effects. One important point remarked by the authors, is that, contrary to the general opinion, the enhancement of the Figure of Merit will not come from an increment in the Seebeck coefficient. Instead, this would be due to an increment of the electrical conductivity, which can be greatly enhanced in certain crystalline orientations. In this way, the mentioned surface roughness scattering of the carriers would be overcome.

4. Devices

As it usually happens when fundamental research approaches to applied research, money has the last word in the research lines that will lead to the development of a final device with real possibilities to enter in the market. Therefore, in order to have competitive costs in the energy obtained by thermoelectric generation, the thermoelectric devices must be as cheap as possible, that is, it is necessary to find a way to increase their efficiency without increasing their total cost. This could be done, for instance, selecting the thermoelectric compounds with cheaper elements. To be more precise, the target cost obtained from this energy harvesting should be around 1–2 €/W to make them competitive with other energy sources. However, as shown by Salzeber et al. [50], the corresponding costs related to the thermoelectric materials in the production of a thermoelectric device based in Skutterudites is just a ~25%, and the manufacturing process a ~50% of the total cost (see Fig. 10). This means that, not only the composition of the thermoelectric module should be inexpensive, but it also must be easy to handle in the industry. Therefore, more effort has to be made in improving the architecture of the devices themselves. Moreover, improvements in the electrical and thermal contacts are mandatory to minimize losses and, consequently, increase the performance (efficiency) of the final device.

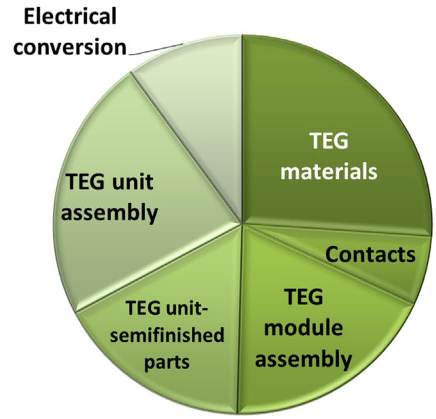


Fig. 10. Cost assessment for a thermoelectric energy generator (TEG) unit for mass production (adapted from Ref. [50]).

5. Conclusions

In summary, in this review it has been shown that the efficiency of thermoelectric materials has been highly improved in recent years, clearly surpassing the level of $ZT = 1$ obtained in classical bulk materials. In this sense, the increasing know–how on the preparation of nano-structures (not only reducing their size but also tailoring such reduction) has been demonstrated to be a powerful tool to achieve record efficiencies.

These improvements in the thermoelectric performance provoked by nano-structuring, however, have been mainly due to the reduction of the thermal conductivity. Although this is a success in itself, the enhanced properties from the nano-structuration were expected to come also from the improvement of the power factor, as it was predicted theoretically. The lack of experimental success in its improvement, together with very recent theoretical predictions that shadow the expectations of enhancing the Seebeck coefficient, makes it necessary to increase the efforts to understand the underlying physics of thermoelectricity at the nanoscale (phonon transport and carrier transport, in particular, when the number of interfaces increase or several scattering mechanisms are present). This will be the basis to uncover the real possibilities of the thermoelectric materials for efficient energy generation. Regarding this, we believe that it is of high importance to improve the metrology of thermoelectric nano-structures and to use those measurements as a feedback for further optimization of the nano-compounds. Besides, it is essential to have reproducibility in the results among different laboratories and, to this end, it is also important to have well established reference samples, as well as to improve the (electrical and thermal) contact resistance.

Moreover, there is a wide range of thermoelectric materials where a huge enhancement of *ZT* has been achieved in the last decade. This further encourages the search for further improvements which, eventually, may lead to higher performance devices. Nevertheless, the engineering aspects of thermoelectric device fabrication (design, contacts, and interfacial materials) are still a rather unexplored field where much improvement should also be achieved during this century to make them competitive.

Acknowledgment

Authors want to thank the ERC 2008 Starting Grant Nano-TEC number 240497 for financial support.

References

[1] Agency EE Energy and environment report 2008; 2008.
[2] Commision IE Efficient electrical energy transmission and distribution; 2007.
[3] Bubnova O, Khan ZU, Malti A, Braun S, Fahlman M, Berggren M, et al. Optimization of the thermoelectric figure of merit in the conducting polymer poly(3,4-ethylenedioxythiophene). Nature Materials 2011;10:429–33.
[4] Tang J, Wang H-T, Lee DH, Fardy M, Huo Z, Russell TP, et al. Holey silicon as an efficient thermoelectric material. Nano Letters 2010;10:4279–83.
[5] Snyder GJ, Toberer ES. Complex thermoelectric materials. Nature Materials 2008;7:105–14.
[6] Ares JR, Jiménez Ferrer I, Díaz-Chao P, Clamagirand JM, Yoda S, Carcelén V, et al. Termoelectricidad: Orígenes, fenomenología y materiales alternativos. Revista Española de Física 2012:26.
[7] Eilertsen J, Li J, Rouvimov S, Subramanian MA. Thermoelectric properties of indium-filled $InxRh_4Sb_{12}$ skutterudites. Journal of Alloys and Compounds 2011;509:6289–95.

[8] Dresselhaus MS, Chen G, Tang MY, Yang RG, Lee H, Wang DZ, et al. New Directions for Low-Dimensional Thermoelectric Materials. Advanced Materials 2007;19:1043–53.
[9] Heremans JP, Wiendlocha B, Chamoire AM. Resonant levels in bulk thermoelectric semiconductors. Energy & Environmental Science 2012;5:5510–30.
[10] Sootsman JR, Chung DY, Kanatzidis MG. New and old concepts in thermoelectric materials. Angewandte Chemie International Edition 2009;48:8616–39.
[11] Kanatzidis MG. Nanostructured thermoelectrics: the new paradigm? Chemistry of Materials 2009;22:648–59.
[12] Nolas GS, Poon J, Kanatzidis M. Recent developments in bulk thermoelectric materials. MRS Bulletin 2006;31:199–205.
[13] Rao AM, Ji X, Tritt TM. Properties of nanostructured one-dimensional and composite thermoelectric materials. MRS Bulletin 2006;31:218–23.
[14] Böttner H, Chen G, Venkatasubramanian R. Aspects of thin-film superlattice thermoelectric materials, devices, and applications. MRS Bulletin 2006;31: 211–7.
[15] Zhang G, Li B. Impacts of doping on thermal and thermoelectric properties of nanomaterials. Nanoscale 2010;2:1058–68.
[16] Vineis CJ, Shakouri A, Majumdar A, Kanatzidis MG. Nanostructured thermoelectrics: big efficiency gains from small features. Advanced Materials 2010;22:3970–80.
[17] Majumdar A. Thermoelectricity in semiconductor nanostructures. Science 2004;303:777–8.
[18] Pichanusakorn P, Bandaru P. Nanostructured thermoelectrics. Materials Science and Engineering: R: Reports 2010;67:19–63.
[19] Minnich AJ, Dresselhaus MS, Ren ZF, Chen G. Bulk nanostructured thermoelectric materials: current research and future prospects. Energy & Environmental Science 2009;2:466–79.
[20] Zebarjadi M, Esfarjani K, Dresselhaus MS, Ren ZF, Chen G. Perspectives on thermoelectrics: from fundamentals to device applications. Energy & Environmental Science 2012;5:5147–62.
[21] Hicks LD, Dresselhaus MS. Effect of quantum-well structures on the thermoelectric figure of merit. Physical Review B. 1993;47:12727–31.
[22] Hicks LD, Harman TC, Sun X, Dresselhaus MS. Experimental study of the effect of quantum-well structures on the thermoelectric figure of merit. Physical Review B. 1996;53:R10493.
[23] Medlin DL, Snyder GJ. Interfaces in bulk thermoelectric materials: a review for current opinion in colloid and interface science. Current Opinion in Colloid & Interface Science 2009;14:226–35.
[24] Yang R, Chen G. Thermal conductivity modeling of periodic two-dimensional nanocomposites. Physical Review B. 2004;69:195316.
[25] Bux SK, Fleurial J-P, Kaner RB. Nanostructured materials for thermoelectric applications. Chemical Communications 2010;46:8311–24.
[26] Lan Y, Minnich AJ, Chen G, Ren Z. Enhancement of thermoelectric figure-of-merit by a bulk nanostructuring approach. Advanced Functional Materials 2010;20:357–76.
[27] Joshi G, Lee H, Lan Y, Wang X, Zhu G, Wang D, et al. Enhanced thermoelectric Figure-of-Merit in nanostructured p-type silicon germanium bulk alloys. Nano Letters 2008;8:4670–4.
[28] Wang XW, Lee H, Lan YC, Zhu GH, Joshi G, Wang DZ, et al. Enhanced thermoelectric figure of merit in nanostructured n-type silicon germanium bulk alloy. Applied Physics Letters 2008;93:193121.
[29] Zhao LD, Zhang BP, Li JF, Zhang HL, Liu WS. Enhanced thermoelectric and mechanical properties in textured n-type Bi_2Te_3 prepared by spark plasma sintering. Solid State Sciences 2008;10:651–8.
[30] Scheele M, Oeschler N, Meier K, Kornowski A, Klinke C, Weller H. Synthesis and thermoelectric characterization of Bi_2Te_3 nanoparticles. Advanced Functional Materials 2009;19:3476–83.
[31] Poudel B, Hao Q, Ma Y, Lan Y, Minnich A, Yu B, et al. High-thermoelectric performance of nanostructured bismuth antimony telluride bulk alloys. Science 2008;320:634–8.
[32] Xie W, Tang X, Yan Y, Zhang Q, Tritt TM. High thermoelectric performance BiSbTe alloy with unique low-dimensional structure. Journal of Applied Physics 2009;105:113713–8.
[33] Lv HY, Liu HJ, Pan L, Wen YW, Tan XJ, Shi J, et al. Enhanced thermoelectric performance of $(Sb_{0.75}Bi_{0.25})2Te_3$ compound from first-principles calculations. Applied Physics Letters 2010;96(142101)–3 2010;96(142101).
[34] Heremans JP, Thrush CM, Morelli DT. Thermopower enhancement in lead telluride nanostructures. Physical Review B. 2004;70:115334.
[35] Heremans JP, Thrush CM, Morelli DT. Thermopower enhancement in PbTe with Pb precipitates. Journal of Applied Physics 2005;98:063703.
[36] Heremans J. Nanometer-scale thermoelectric materials. In: Bhushan B, editor. Springer Handbook of nanotechnology. Berlin, Heidelberg: Springer; 2007. p. 345–74.
[37] Martin J, Nolas GS, Zhang W, Chen L. PbTe nanocomposites synthesized from PbTe nanocrystals. AIP; 2007.
[38] Heremans JP, Jovovic V, Toberer ES, Saramat A, Kurosaki K, Charoenphakdee A, et al. Enhancement of thermoelectric efficiency in PbTe by distortion of the electronic density of states. Science 2008;321:554–7.
[39] Girard SN, He J, Zhou X, Shoemaker D, Jaworski CM, Uher C, et al. High performance Na-doped PbTe–PbS thermoelectric materials: electronic density of states modification and shape-controlled nanostructures. Journal of the American Chemical Society 2011;133:16588–97.
[40] Pei Y, Shi X, LaLonde A, Wang H, Chen L, Snyder GJ. Convergence of electronic bands for high performance bulk thermoelectrics. Nature 2011;473:66–9.
[41] Wang H, Li J-F, Zou M, Sui T. Synthesis and transport property of $AgSbTe_2$ as a promising thermoelectric compound. Applied Physics Letters 2008;93: 202106.
[42] Xu J, Li H, Du B, Tang X, Zhang Q, Uher C. High thermoelectric figure of merit and nanostructuring in bulk $AgSbTe_2$. Journal of Materials Chemistry 2010;20:6138–43.
[43] Du B, Li H, Xu J, Tang X, Uher C. Enhanced thermoelectric performance and novel nanopores in $AgSbTe_2$ prepared by melt spinning. Journal of Solid State Chemistry 2011;184:109–14.
[44] Hsu KF, Loo S, Guo F, Chen W, Dyck JS, Uher C, et al. Cubic $AgPbmSbTe_2+m$: bulk thermoelectric materials with high Figure of Merit. Science 2004;303:818–21.
[45] Wang H, Li J-F, Nan C-W, Zhou M, Liu W, Zhang B-P, et al. High-performance $Ag_{0.8}Pb_{(18+x)}SbTe_{20}$ thermoelectric bulk materials fabricated by mechanical alloying and spark plasma sintering. Applied Physics Letters 2006;88:092104.
[46] Cai KF, Yan C, He ZM, Cui JL, Stiewe C, Müller E, et al. Preparation and thermoelectric properties of $AgPbmSbTe_2+m$ alloys. Journal of Alloys and Compounds 2009;469:499–503.
[47] Chen N, Gascoin F, Snyder GJ, Muller E, Karpinski G, Stiewe C. Macroscopic thermoelectric inhomogeneities in $(AgSbTe_2)xPbTe_1x$. Applied Physics Letters 2005;87(171903)–3 2005;87(171903).
[48] Poudeu PFP, D'Angelo J, Downey AD, Short JL, Hogan TP, Kanatzidis MG. High thermoelectric Figure of Merit and nanostructuring in bulk p-type $Na_{1-x}PbmSb_yTem_{+2}$. Angewandte Chemie 2006;118:3919–23.
[49] PFP Poudeu, Guéguen AL, Wu C-I, Hogan T, Kanatzidis MG. High Figure of Merit in nanostructured n-type KPbmSbTem+2 thermoelectric materials†. Chemistry of Materials 2009;22:1046–53.
[50] Salzgeber K, Prenninger P, Grytsiv A, Rogl P, Bauer E. Skutterudites: thermoelectric materials for automotive applications? Journal of Electronic Materials 2010;39:2074–8.
[51] Tang X, Zhang Q, Chen L, Goto T, Hirai T. Synthesis and thermoelectric properties of p-type- and n-type-filled skutterudite $RyMxCo_{(4-x)}Sb_{12}$(R:Ce, Ba,Y;M:Fe,Ni). Journal of Applied Physics 2005;97:093712.
[52] Shi X, Yang J, Salvador JR, Chi M, Cho JY, Wang H, et al. Multiple-filled skutterudites: high thermoelectric Figure of Merit through separately optimizing electrical and thermal transports. Journal of the American Chemical Society 2011;133:7837–46.
[53] Li H, Tang X, Zhang Q, Uher C. High performance $InxCeyCo_4Sb_{12}$ thermoelectric materials with in situ forming nanostructured InSb phase. Applied Physics Letters 2009;94:102114.
[54] Mi JL, Zhu TJ, Zhao XB, Ma J. Nanostructuring and thermoelectric properties of bulk skutterudite compound $CoSb_3$. Journal of Applied Physics 2007;101:054314.
[55] He Q, Hu S, Tang X, Lan Y, Yang J, Wang X, et al. The great improvement effect of pores on ZT in $Co_{(1-x)}Ni\ _xSb_3$ system. Applied Physics Letters 2008;93:042108.
[56] Shi X, Chen L, Yang J, Meisner GP. Enhanced thermoelectric figure of merit of $CoSb_3$ via large-defect scattering. Applied Physics Letters 2004;84:3.
[57] He J, Liu Y, Funahashi R. Oxide thermoelectrics: the challenges, progress, and outlook. Cambridge, Royaume-Uni: Cambridge University Press; 2011.
[58] Culp SR, Poon SJ, Hickman N, Tritt TM, Blumm J. Effect of substitutions on the thermoelectric figure of merit of half-Heusler phases at 800 °C. Applied Physics Letters 2006;88:042106.
[59] Joshi G, Yan X, Wang H, Liu W, Chen G, Ren Z. Enhancement in thermoelectric Figure-of-Merit of an n-type half-Heusler compound by the nanocomposite approach. Advanced Energy Materials 2011;1:643–7.
[60] Makongo JPA, Misra DK, Zhou X, Pant A, Shabetai MR, Su X, et al. Simultaneous large enhancements in thermopower and electrical conductivity of bulk nanostructured Half-Heusler alloys. Journal of the American Chemical Society 2011;133:18843–52.
[61] Esaki L, Tsu R. Superlattice and negative differential conductivity in semiconductors. IBM Journal of Research and Development 1970;14:61–5.
[62] Koga T, Sun X, Cronin SB, Dresselhaus MS. Carrier pocket engineering to design superior thermoelectric materials using GaAs/AlAs superlattices. AIP; 1998.
[63] Venkatasubramanian R, Colpitts T, Watko E, Lamvik M, El-Masry N. MOCVD of Bi_2Te_3, Sb_2Te_3 and their superlattice structures for thin-film thermoelectric applications. Journal of Crystal Growth 1997;170:817–21.
[64] Venkatasubramanian R, Siivola E, Colpitts T, O'Quinn B. Thin-film thermoelectric devices with high room-temperature figures of merit. London, Royaume-Uni: Nature Publishing Group; 2001.
[65] Beyer H, Nurnus J, Böttner H, Lambrecht A, Wagner E, Bauer G. High thermoelectric figure of merit ZT in PbTe and Bi_2Te_3-based superlattices by a reduction of the thermal conductivity. Physica E: Low-dimensional Systems and Nanostructures 2002;13:965–8.
[66] Harman T, Taylor P, Spears D, Walsh M. Thermoelectric quantum-dot superlattices with high ZT. Journal of Electronic Materials 2000;29: L1–2.
[67] Harman T, Walsh M, laforge B, Turner G. Nanostructured thermoelectric materials. Journal of Electronic Materials. 2005;34:L19–22.
[68] Harman TC, Taylor PJ, Walsh MP, LaForge BE. Quantum dot superlattice thermoelectric materials and devices. Science 2002;297:2229–32.
[69] Ezzahri Y, Zeng G, Fukutani K, Bian Z, Shakouri A. A comparison of thin film microrefrigerators based on Si/SiGe superlattice and bulk SiGe. Microelectronics Journal 2008;39:981–91.

[70] Heremans J, Thrush CM, Zhang Z, Sun X, Dresselhaus MS, Ying JY, et al. Magnetoresistance of bismuth nanowire arrays: a possible transition from one-dimensional to three-dimensional localization. Physical Review B 1998;58:R10091–5.
[71] Zhibo Zhang MSD. Bismuth quantum-wire arrays fabricated by a vacuum melting and pressure injection process. Journal of Materials Research 1998;13:4.
[72] Bejenari I, Kantser V. Thermoelectric properties of bismuth telluride nanowires in the constant relaxation-time approximation. Physical Review B. 2008;78:115322.
[73] Martín J, Maiz J, Sacristan J, Mijangos C. Tailored polymer-based nanorods and nanotubes by "template synthesis": from preparation to applications. Polymer 2012;53:1149–66.
[74] Martín J, Manzano CV, Martín-González M. In-depth study of self-ordered porous alumina in the 140–400 nm pore diameter range. Microporous and Mesoporous Materials 2012;151:311–6.
[75] Jin CG, Jiang GW, Liu WF, Cai WL, Yao LZ, Yao Z, et al. Fabrication of large-area single crystal bismuth nanowire arrays. Journal of Materials Chemistry 2003;13:1743–6.
[76] Hong K, Yang FY, Liu K, Reich DH, Searson PC, Chien CL, et al. Giant positive magnetoresistance of Bi nanowire arrays in high magnetic fields. Journal of Applied Physics 1999;85:6184–6.
[77] Boulanger C. Thermoelectric material electroplating: a historical review. Journal of Electronic Materials 2010;39:1818–27.
[78] Martín-González M, Prieto AL, Gronsky R, Sands T, Stacy AM. High-density 40 nm diameter Sb-rich $Bi_{2-x}Sb_xTe_3$ nanowire arrays. Advanced Materials 2003;15:1003–6.
[79] Vereecken PM, Sun L, Searson PC, Tanase M, Reich DH, Chien CL. Magnetotransport properties of bismuth films on p-GaAs. Journal of Applied Physics 2000;88:6529–35.
[80] Martín-González M, Prieto AL, Knox MS, Gronsky R, Sands T, Stacy AM. Electrodeposition of $Bi_{1-x}Sb_x$ films and 200-nm wire arrays from a nonaqueous solvent. Chemistry of Materials 2003;15:1676–81.
[81] Takahashi M, Katou Y, Nagata K, Furuta S. The composition and conductivity of electrodeposited BiTe alloy films. Thin Solid Films 1994;240:70–2.
[82] Martin-Gonzalez MS, Prieto AL, Gronsky R, Sands T, Stacy AM. Insights into the electrodeposition of Bi_2Te_3. Journal of the Electrochemical Society 2002;149:C546–54.
[83] Liu W, Cai W, Yao L. Electrochemical deposition of well-ordered single-crystal PbTe nanowire arrays. Chemistry Letters 2007;36:1362–3.
[84] Michel S, Stein N, Schneider M, Boulanger C, Lecuire JM. Optimization of chemical and electrochemical parameters for the preparation of n-type Bi2Te2.7Se0.3 thin films by electrodeposition. Journal of Applied Electrochemistry 2003;33:23–7.
[85] Lenoir B, Dauscher A, Cassart M, Ravich YI, Scherrer H. Effect of antimony content on the thermoelectric figure of merit of $Bi_{1-x}Sb_x$ alloys. Journal of Physics and Chemistry of Solids 1998;59:129–34.
[86] Xiao F, Hangarter C, Yoo B, Rheem Y, Lee K-H, Myung NV. Recent progress in electrodeposition of thermoelectric thin films and nanostructures. Electrochimica Acta 2008;53:8103–17.
[87] Sander MS, Gronsky R, Sands T, Stacy AM. Structure of bismuth telluride nanowire arrays fabricated by electrodeposition into porous anodic alumina templates. Chemistry of Materials 2002;15:335–9.
[88] Zhou J, Jin C, Seol JH, Li X, Shi L. Thermoelectric properties of individual electrodeposited bismuth telluride nanowires. Applied Physics Letters 2005;87:133109.
[89] Menke EJ, Brown MA, Li Q, Hemminger JC, Penner RM. Bismuth telluride (Bi_2Te_3) nanowires: synthesis by cyclic electrodeposition/stripping, thinning by electrooxidation, and electrical power generation†. Langmuir 2006;22:10564–74.
[90] Borca-Tasciuc DA, Chen G, Prieto A, Martin-Gonzalez MS, Stacy A, Sands T, et al. Thermal properties of electrodeposited bismuth telluride nanowires embedded in amorphous alumina. Applied Physics Letters 2004;85:6001–3.
[91] Lee J, Kim Y, Cagnon L, Gösele U, Lee J, Nielsch K. Power factor measurements of bismuth telluride nanowires grown by pulsed electrodeposition. physica status solidi (RRL) – Rapid Research Letters 2010;4:43–5.
[92] Chen C-L, Chen Y-Y, Lin S-J, Ho JC, Lee P-C, Chen C-D, et al. Fabrication and Characterization of Electrodeposited Bismuth Telluride Films and Nanowires. The Journal of Physical Chemistry C. 2010;114:3385–9.
[93] Zhao XB, Ji XH, Zhang YH, Zhu TJ, Tu JP, Zhang XB. Bismuth telluride nanotubes and the effects on the thermoelectric properties of nanotube-containing nanocomposites. Applied Physics letters 2005;86:062111.
[94] Boukai AI, Bunimovich Y, Tahir-Kheli J, Yu J-K, Goddard Iii WA, Heath JR. Silicon nanowires as efficient thermoelectric materials. Nature 2008;451: 168–71.
[95] Hochbaum AI, Chen R, Diaz Delgado R, Liang W, Garnett EC, Najarian M, et al. Enhanced thermoelectric performance of rough silicon nanowires. London, Royaume-Uni: Nature Publishing Group; 2008.
[96] Gudiksen MS, Lauhon LJ, Wang J, Smith DC, Lieber CM. Growth of nanowire superlattice structures for nanoscale photonics and electronics. Nature 2002;415:3.
[97] Dames C, Chen G. Theoretical phonon thermal conductivity of Si/Ge superlattice nanowires. AIP; 2004.
[98] Piraux L, George JM, Despres JF, Leroy C, Ferain E, Legras R, et al. Giant magnetoresistance in magnetic multilayered nanowires. Applied Physics Letters 1994;65:2484–6.
[99] Lim JR, Whitacre JF, Fleurial JP, Huang CK, Ryan MA, Myung NV. Fabrication method for thermoelectric nanodevices. Advanced Materials 2005;17:1488–92.
[100] Keyani J, Stacy AM, Sharp J. Assembly and measurement of a hybrid nanowire-bulk thermoelectric device. Melville, NY, Etats-Unis: American Institute of Physics; 2006.
[101] Mavrokefalos A, Moore AL, Pettes MT, Shi L, Wang W, Li X. Thermoelectric and structural characterizations of individual electrodeposited bismuth telluride nanowires. Journal of Applied Physics 2009;105:104318.
[102] Wu Y, Fan R, Yang P. Block-by-block growth of single-crystalline Si/SiGe superlattice nanowires. Nano Letters 2002;2:83–6.
[103] Li D, Wu Y, Fan R, Yang P, Majumdar A. Thermal conductivity of Si/SiGe superlattice nanowires. Applied Physics Letters 2003;83:3186–8.
[104] Kim R, Datta S, Lundstrom MS. Influence of dimensionality on thermoelectric device performance. Journal of Applied Physics 2009;105:034506.
[105] Yu J-K, Mitrovic S, Tham D, Varghese J, Heath JR. Reduction of thermal conductivity in phononic nanomesh structures. Nature Nanotechnology 2010;5:718–21.
[106] Hopkins PE, Reinke CM, Su MF, Olsson RH, Shaner EA, Leseman ZC, et al. Reduction in the thermal conductivity of single crystalline silicon by phononic crystal patterning. Nano Letters 2010;11:107–12.
[107] Dechaumphai E, Chen R. Thermal transport in phononic crystals: the role of zone folding effect. Journal of Applied Physics 2012;111:073508-8.
[108] Mehta RJ, Zhang Y, Karthik C, Singh B, Siegel RW, Borca-Tasciuc T, et al. A new class of doped nanobulk high-figure-of-merit thermoelectrics by scalable bottom-up assembly. Nature Materials 2012;11:233–40.
[109] Zuzok R, Kaiser AB, Pukacki W, Roth S. Thermoelectric power and conductivity of iodine-doped "new" polyacetylene. The Journal of Chemical Physics 1991;95:1270–5.
[110] Li J, Tang X, Li H, Yan Y, Zhang Q. Synthesis and thermoelectric properties of hydrochloric acid-doped polyaniline. Synthetic Metals 2010;160:1153–8.
[111] Dubey N, Leclerc M. Conducting polymers: efficient thermoelectric materials. Journal of Polymer Science Part B: Polymer Physics 2011;49:467–75.
[112] Bounioux C, Díaz-Chao P, Campoy-Quiles M, Martín-González MS, Goñi AR, Yerushalmi-Rozen R, et al. Thermoelectric composites of poly (3-hexylthiophene) and carbon nanotubes with a large power factor. Energy & Environmental Science 2013;6:918–25.
[113] Shirakawa H, Louis EJ, MacDiarmid AG, Chiang CK, Heeger AJ. Synthesis of electrically conducting organic polymers: halogen derivatives of polyacetylene, (CH). Journal of the Chemical Society, Chemical Communications 1977:578–80.
[114] Epstein AJ, Ginder JM, Zuo F, Bigelow RW, Woo HS, Tanner DB, et al. Insulator-to-metal transition in polyaniline. Synthetic Metals 1987;18:303–9.
[115] Hostler SR, Kaul P, Day K, Qu V, Cullen C, Abramson AR, et al. Thermal and electrical characterization of nanocomposites for thermoelectrics. In: 2006 ITHERM '06. The tenth intersociety conference on thermal and thermomechanical phenomena in electronics systems; 2006;6:1405.
[116] Yan H, Ohta T, Toshima N. Stretched polyaniline films doped by (±)–10-camphorsulfonic acid: anisotropy and improvement of thermoelectric properties. Macromolecular Materials and Engineering 2001;286:139–42.
[117] Yang Y, Lee K, Mielczarek K, Hu W, Zakhidov A. Nanoimprint of dehydrated PEDOT:PSS for organic photovoltaics. Nanotechnology 2011;22:485301.
[118] Latessa G, Brunetti F, Reale A, Saggio G, Di Carlo A. Piezoresistive behaviour of flexible PEDOT:PSS based sensors. Sensors and Actuators B: Chemical 2009;139:304–9.
[119] Xiao Y, Cui X, Martin DC. Electrochemical polymerization and properties of PEDOT/S-EDOT on neural microelectrode arrays. Journal of Electroanalytical Chemistry 2004;573:43–8.
[120] Garreau S, Louam G, Lefrant S, Buisson JP, Froyer G. Optical study and vibrational analysis of the poly (3,4-ethylenedioxythiophene) (PEDT). Synthetic Metals 1999;101:312–3.
[121] Scholdt M, Do H, Lang J, Gall A, Colsmann A, Lemmer U, et al. Organic semiconductors for thermoelectric applications. Journal of Electronic Materials 2010;39:1589–92.
[122] Zhao XB, Hu SH, Zhao MJ, Zhu TJ. Thermoelectric properties of $Bi_{0.5}Sb_{1.5}Te_3$/polyaniline hybrids prepared by mechanical blending. Materials Letters 2002;52:147–9.
[123] Wang L, Wang D, Zhu G, Li J, Pan F. Thermoelectric properties of conducting polyaniline/graphite composites. Materials Letters 2011;65:1086–8.
[124] Wang Y, Cai K, Yin J, An B, Du Y, Yao X. In situ fabrication and thermoelectric properties of PbTe–polyaniline composite nanostructures. Journal of Nanoparticle Research 2011;13:533–9.
[125] See KC, Feser JP, Chen CE, Majumdar A, Urban JJ, Segalman RA. Water-processable polymer-nanocrystal hybrids for thermoelectrics. Nano Letters 2010;10:4664–7.
[126] Zhang B, Sun J, Katz HE, Fang F, Opila RL. Promising thermoelectric properties of commercial PEDOT:PSS materials and their Bi_2Te_3 powder composites. ACS Applied Materials & Interfaces 2010;2:3170–8.
[127] Ao W, Wang L, Li J, Pan F, Wu C. Synthesis and characterization of polythiophene/Bi_2Te_3 nanocomposite thermoelectric material. Journal of Electronic Materials 2011;40:2027–32.
[128] Yu C, Kim YS, Kim D, Grunlan JC. Thermoelectric behavior of segregated-network polymer nanocomposites. Nano Letters 2008;8:4428–32.
[129] Yu C, Choi K, Yin L, Grunlan JC. Light-weight flexible carbon nanotube based organic composites with large thermoelectric power factors. ACS Nano 2011;5:7885–92.
[130] Meng C, Liu C, Fan SA. Promising approach to enhanced thermoelectric properties using carbon nanotube networks. Advanced Materials 2010;22: 535–9.

[131] Yao Q, Chen L, Zhang W, Liufu S, Chen X. Enhanced Thermoelectric Performance of Single-Walled Carbon Nanotubes/Polyaniline Hybrid Nanocomposites. ACS Nano 2010;4:2445–51.
[132] Kim D, Kim Y, Choi K, Grunlan JC, Yu C. Improved thermoelectric behavior of nanotube-filled polymer composites with poly(3,4-ethylenedioxythiophene) poly(styrenesulfonate). ACS Nano 2009;4:513–23.
[133] Tessler N, Preezant Y, Rappaport N, Roichman Y. Charge transport in disordered organic materials and its relevance to thin-film devices: a tutorial review. Advanced Materials 2009;21:2741–61.
[134] Reddy P, Jang S-Y, Segalman RA, Majumdar A. Thermoelectricity in molecular junctions. Science 2007;315:1568–71.
[135] Enrique M. Thermoelectric power and electrical conductance of DNA based molecular junctions. Nanotechnology 2005;16:S254.
[136] Maciá E. DNA-based thermoelectric devices: a theoretical prospective. Physical Review B. 2007;75:035130.
[137] Hatsopoulos GN, Kaye J. Measured thermal efficiencies of a diode configuration of a thermo electron engine. Journal of Applied Physics 1958;29:1124–5.
[138] Mahan GD. Thermionic refrigeration. Journal of Applied Physics. 1994;76:4362–6.
[139] Shakouri A, Bowers JE. Heterostructure integrated thermionic coolers. Applied Physics Letters 1997;71:1234–6.
[140] Vashaee D, Shakouri A. Improved thermoelectric power factor in metal-based superlattices. Physical Review Letters 2004;92:106103.
[141] Radtke RJ, Ehrenreich H, Grein CH. Multilayer thermoelectric refrigeration in $Hg_{(1-x)}Cd_xTe$ superlattices. Journal of Applied Physics 1999;86:3195–8.
[142] Ulrich MD, Barnes PA, Vining CB. Comparison of solid-state thermionic refrigeration with thermoelectric refrigeration. Journal of Applied Physics 2001;90:1625–31.
[143] Rawat V, Koh YK, Cahill DG, Sands TD. Thermal conductivity of (Zr,W)N/ScN metal/semiconductor multilayers and superlattices. Journal of Applied Physics 2009;105:024909.
[144] Su L, Gan YX. Advances in thermoelectric energy conversion nanocomposites. Advances in Composite Materials for Medicine and Nanotechnology 2011.
[145] Kauzlarich SM, Brown SR, Jeffrey Snyder G. Zintl phases for thermoelectric devices. Dalton Transactions 2007:2099–107.
[146] Toberer ES, May AF, Snyder GJ. Zintl chemistry for designing high efficiency thermoelectric materials†‡. Chemistry of Materials 2009;22:624–34.
[147] Caillat T, Fleurial JP, Borshchevsky A. Preparation and thermoelectric properties of semiconducting Zn_4Sb_3. Journal of Physics and Chemistry of Solids 1997;58:1119–25.
[148] Pedersen BL, Iversen BB. Thermally stable thermoelectric Zn_4Sb_3 by zone-melting synthesis. Applied Physics Letters 2008;92:161907.
[149] Schlecht S, Erk C, Yosef M. Nanoscale zinc antimonides: synthesis and phase stability. Inorganic Chemistry. 2006;45:1693–7.
[150] Pedersen BL, Birkedal H, Iversen BB, Nygren M, Frederiksen PT. Influence of sample compaction on the thermoelectric performance of Zn4Sb3. Applied Physics Letters 2006;89:242108.
[151] Wang S, Li H, Qi D, Xie W, Tang X. Enhancement of the thermoelectric performance of β-Zn_4Sb_3 by in situ nanostructures and minute Cd-doping. Acta Materialia 2011;59:4805–17.
[152] Bjerg L, Madsen GKH, Iversen BB. Enhanced thermoelectric properties in zinc antimonides. Chemistry of Materials 2011;23:3907–14.
[153] Gascoin F, Ottensmann S, Stark D, Haïle SM, Snyder GJ. Zintl phases as thermoelectric materials: tuned transport properties of the compounds $Ca_xYb_{1-x}Zn_2Sb_2$. Advanced Functional Materials 2005;15:1860–4.
[154] Toberer ES, May AF, Melot BC, Flage-Larsen E, Snyder GJ. Electronic structure and transport in thermoelectric compounds AZn_2Sb_2 (A=Sr, Ca, Yb, Eu). Dalton Transactions 2010:39.
[155] Wang X-J, Tang M-B, Chen H-H, Yang X-X, Zhao J-T, Burkhardt U, et al. Synthesis and high thermoelectric efficiency of Zintl phase $YbCd_{(2-x)}Zn_xSb_2$. Applied Physics Letters 2009;94:092106.
[156] Gravier L, Serrano-Guisan S, Reuse F, Ansermet JP. Spin-dependent Peltier effect of perpendicular currents in multilayered nanowires. Physical Review B 2006;73:052410.
[157] Uchida K, Takahashi S, Harii K, Ieda J, Koshibae W, Ando K, et al. Observation of the spin Seebeck effect. Nature 2008;455:778–81.
[158] Jaworski CM, Yang J, Mack S, Awschalom DD, Heremans JP, Myers RC. Observation of the spin-Seebeck effect in a ferromagnetic semiconductor. Nature Materials 2010;9:898–903.
[159] Uchida K, Xiao J, Adachi H, Ohe J, Takahashi S, Ieda J, et al. Spin Seebeck insulator. Nature Materials 2010;9:894–7.
[160] Jaworski CM, Yang J, Mack S, Awschalom DD, Myers RC, Heremans JP. Spin-Seebeck effect: a phonon driven spin distribution. Physical Review Letters 2011;106:186601.
[161] Cornett JE, Rabin O. Thermoelectric figure of merit calculations for semiconducting nanowires. Applied Physics Letters 2011;98:182104.
[162] Cornett JE, Rabin O. Universal scaling relations for the thermoelectric power factor of semiconducting nanostructures. Physical Review B 2011;84:205410.
[163] Neophytou N, Kosina H. Effects of confinement and orientation on the thermoelectric power factor of silicon nanowires. Physical Review B 2011;83:245305.
[164] Neophytou N, Kosina H. Thermoelectric properties of scaled silicon nanowires using the $sp_3d_5s^*$–SO atomistic tight-binding model and Boltzmann transport. Journal of Electronic Materials 2011;40:753–8.
[165] Neophytou N., Kosina H. On the interplay between Electrical Conductivity and Seebeck Coefficient in Ultra-Narrow Silicon Nanowires, Journal of Electronic Materials 2012;41:1305–11.
[166] Boukai A, Xu K, Heath JR. Size-dependent transport and thermoelectric properties of individual polycrystalline bismuth nanowires. Advanced Materials 2006;18:864–9.
[167] Lin Y-M, Sun X, Dresselhaus MS. Theoretical investigation of thermoelectric transport properties of cylindrical Bi nanowires. Physical Review B 2000;62:4610–23.
[168] Sun X, Zhang Z, Dresselhaus MS. Theoretical modeling of thermoelectricity in Bi nanowires. Applied Physics Letters 1999;74:4005–7.
[169] Liu K, Chien CL, Searson PC. Finite-size effects in bismuth nanowires. Physical Review B 1998;58:R14681–4.
[170] Liu K, Chien CL, Searson PC, Yu-Zhang K. Structural and magneto-transport properties of electrodeposited bismuth nanowires. Applied Physics Letters 1998;73:1436–8.
[171] Li L, Zhang Y, Li GH, Song WH, Zhang LD. A new routine to fabricate Bi single crystalline tapering junction nanowire arrays. Applied Physics A: Materials Science & Processing 2005;80:1053–5.
[172] Xu X, Chen L, Wang C, Yao Q, Feng C. Template synthesis of heterostructured polyaniline/Bi_2Te_3 nanowires. Journal of Solid State Chemistry 2005;178:2163–6.
[173] Li L, Zhang Y, Li G, Zhang L. A route to fabricate single crystalline bismuth nanowire arrays with different diameters. Chemical Physics Letters 2003;378:244–9.
[174] Jin C, Zhang G, Qian T, Li X, Yao Z. Large-area Sb_2Te_3 nanowire arrays. The Journal of Physical Chemistry B 2005;109:1430–2.
[175] Lin Y-M, Rabin O, Cronin SB, Ying JY, Dresselhaus MS. Semimetal–semiconductor transition in $Bi_{(1-x)}Sb_x$ alloy nanowires and their thermoelectric properties. Applied Physics Letters 2002;81:2403–5.
[176] Prieto AL, Martín-González M, Keyani J, Gronsky R, Sands T, Stacy AM. The electrodeposition of high-density, ordered arrays of $Bi_{1-x}Sb_x$ nanowires. Journal of the American Chemical Society 2003;125:2388–9.
[177] Xue FH, Fei GT, Wu B, Cui P, Zhang LD. Direct electrodeposition of highly dense Bi/Sb superlattice nanowire arrays. Journal of the American Chemical Society 2005;127:15348–9.
[178] Müller S, Schötz C, Picht O, Sigle W, Kopold P, Rauber M, et al. Electrochemical synthesis of $Bi_{1-x}Sb_x$ nanowires with simultaneous control on size, composition, and surface roughness. Crystal Growth & Design 2011;12:615–21.
[179] Sapp SA, Lakshmi BB, Martin CR. Template synthesis of bismuth telluride nanowires. Advanced Materials 1999;11:402–4.
[180] Prieto AL, Sander MS, Martín-González MS, Gronsky R, Sands T, Stacy AM. Electrodeposition of ordered Bi_2Te_3 nanowire arrays. Journal of the American Chemical Society 2001;123:7160–1.
[181] Sander MS, Prieto AL, Gronsky R, Sands T, Stacy AM. Fabrication of high-density, high aspect ratio, large-area bismuth telluride nanowire arrays by electrodeposition into porous anodic alumina templates. Advanced Materials 2002;14:665–7.
[182] Martín J, Manzano CV, Caballero-Calero O, Martín-González M. High-aspect-ratio and highly ordered 15-nm porous alumina templates. ACS Applied Materials & Interfaces 2012;5:72–9.
[183] Picht O, Müller S, Alber I, Rauber M, Lensch-Falk J, Medlin DL, et al. Tuning the geometrical and crystallographic characteristics of Bi_2Te_3 nanowires by electrodeposition in ion-track membranes. The Journal of Physical Chemistry C 2012;116:5367–75.
[184] Liang L, Youwen Y, Xiaohu H, Guanghai L, Lide Z. Pulsed electrodeposition of single-crystalline Bi_2Te_3 nanowire arrays. Nanotechnology 2006;17:1706.
[185] Yoo B, Xiao F, Bozhilov KN, Herman J, Ryan MA, Myung NV. Electrodeposition of thermoelectric superlattice nanowires. Advanced Materials 2007;19:296–299.
[186] Martín-González M, Snyder GJ, Prieto AL, Gronsky R, Sands T, Stacy AM. Direct electrodeposition of highly dense 50 nm $Bi_2Te_{3-y}Se_y$ nanowire arrays. Nano Letters 2003;3:973–7.
[187] Behnke J.F., Prieto A.L., Stacy A.M., Sands T. Electrodeposition of $CoSb_3$ nanowires. 1999 Eighteenth international conference on thermoelectrics; 1999. p. 451–3.
[188] Chen L, Hu H, Li Y, Chen G, Yu S, Wu G. Ordered $CoSb_3$ nanowire arrays synthesized by electrodeposition. Chemistry Letters 2006;35:170–1.
[189] Yang Y, Kung SC, Taggart DK, Xiang C, Yang F, Brown MA, et al. Synthesis of PbTe nanowire arrays using lithographically patterned nanowire electrodeposition. Nano Letters 2008;8:2447–51.
[190] Sima M, Enculescu I, Visan T, Spohr R, Trautmann C. Electrochemical deposition of $PbSe_{1-x}Te_x$ nanorod arrays using ion track etched membranes as template. Molecular Crystals and Liquid Crystals 2004;418:21–7.
[191] Mingo N. Thermoelectric figure of merit and maximum power factor in III–V semiconductor nanowires. Applied Physics Letters 2004;84:2652–4.
[192] Zhang X, Hao Y, Meng G, Zhang L. Fabrication of highly ordered InSb nanowire arrays by electrodeposition in porous anodic alumina membranes. Journal of the Electrochemical Society 2005;152:C664–8.